WMO Statement on the State of the Global Climate in 2019

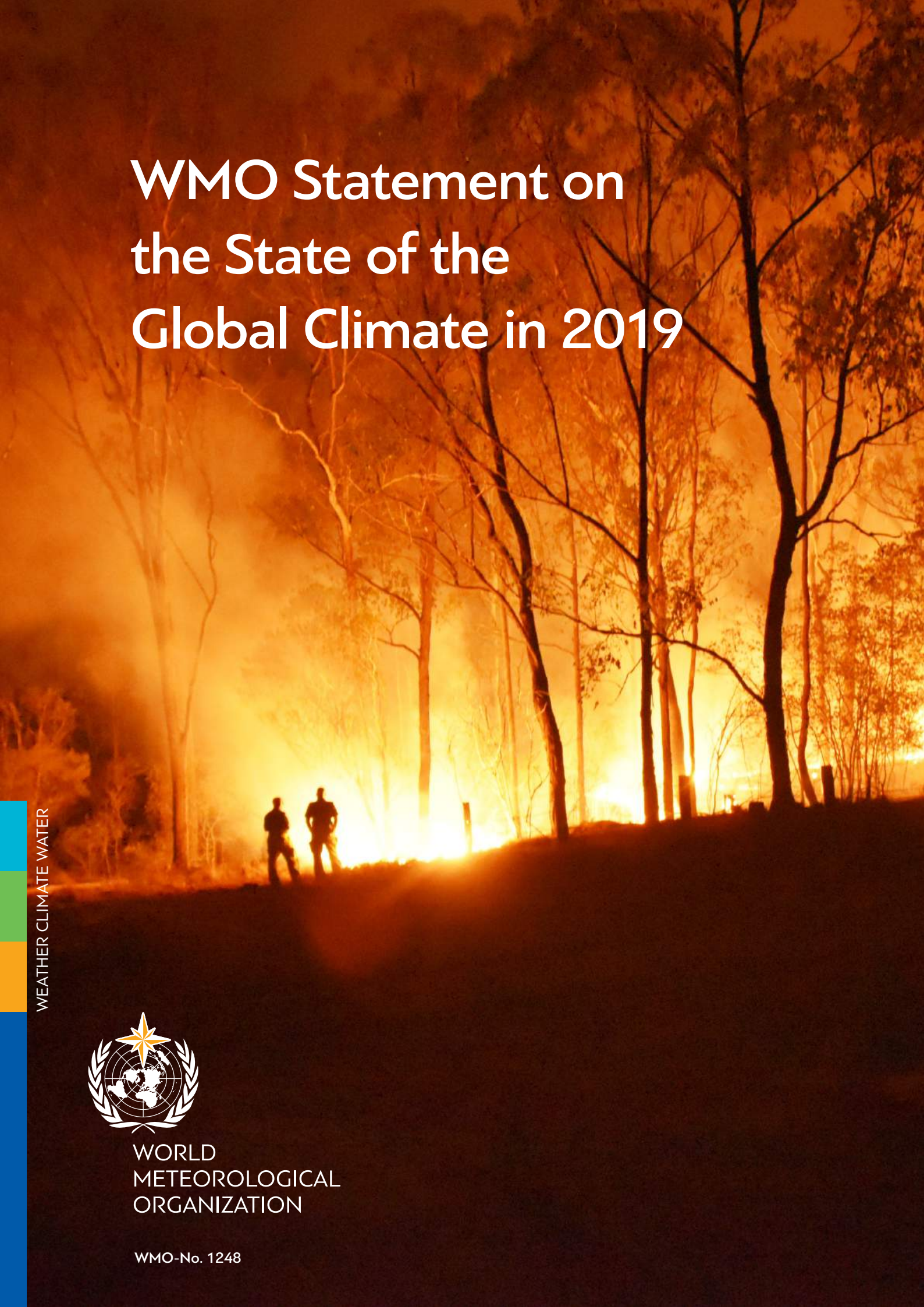

WEATHER CLIMATE WATER

WORLD METEOROLOGICAL ORGANIZATION

WMO-No. 1248

WMO-No. 1248

Chair, Publications Board
World Meteorological Organization (WMO)
7 bis, avenue de la Paix
P.O. Box 2300
CH-1211 Geneva 2, Switzerland

Tel.: +41 (0) 22 730 84 03
Fax: +41 (0) 22 730 81 17
Email: publications@wmo.int

ISBN 978-92-62-11248-5

Cover illustration: Volunteer firefighters rescuing lives and farms from bushfire in Bundaberg, Queensland (Australia).

Contents

Since 2016, the following United Nations agencies have significantly contributed to the WMO Statement on the State of the Global Climate in support of climate policy and action:

Food and Agriculture Organization of the United Nations (FAO),

Intergovernmental Oceanographic Commission of the United Nations Educational, Scientific and Cultural Organization (IOC/UNESCO),

International Monetary Fund (IMF),

International Organization for Migration (IOM),

United Nations Conference on Trade and Development (UNCTAD),

United Nations Environment Programme (UNEP),

Office of the United Nations High Commissioner for Refugees (UNHCR),

United Nations Office for Disaster Risk Reduction (UNDRR),

World Health Organisation (WHO).

Foreword

Concentrations of greenhouse gases, particularly CO_2, continue to rise. The year 2019 ended with a global average temperature of 1.1 °C above estimated pre-industrial averages, second only to the record set in 2016. Without the role of El Niño in the warming increase observed in 2016, 2019 would have been a record year.

Temperature is one indicator of the ongoing climate change. Also, sea levels are rising at an increasing pace, through greater warming of the oceans, on the surface and in the depths, and through the enhanced melting of Greenland's ice and of glaciers, exposing coastal areas and islands to a greater risk of flooding and the submersion of low-lying areas.

Furthermore, in 2019, heatwaves, combined with long periods of drought, were linked to wildfires of unprecedented size. This was the case in Australia, where millions of hectares were set ablaze, and in Siberia and other Arctic regions hit by wildfires of record intensity.

Besides these powerful phenomena, there has been weather-related damage, such as the effects of multi-annual droughts on the internal and cross-border migration of populations, greater exposure of the world population to health hazards due to heat and pollution, and the reduction of economic growth, especially in developing economies, due to rising temperatures and weather extremes.

The results of this report demonstrate that climate change is already very visible in various ways. More ambitious climate mitigation efforts are needed to keep the warming below 2 °C by the end of the century.

The World Meteorological Organization will continue to follow closely climate variability and change and their impact. An information portal is being set up to allow indicators of the state of the climate to be tracked.

I would like to thank the many expert teams in climatology and other disciplines, National Meteorological and Hydrological Services, the global and regional centres for climate data collection and analysis and the United Nations sister agencies. Thanks to their unfailing collaboration, the WMO Statement on the State of the Global Climate has become a flagship publication providing policymakers all over the world with essential climate information.

(P. Taalas)
Secretary-General

Statement by the United Nations Secretary-General

Climate change is the defining challenge of our time. Time is fast running out for us to avert the worst impacts of climate disruption and protect our societies from the inevitable impacts to come.

Science tells us that, even if we are successful in limiting warming to 1.5 °C, we will face significantly increased risks to natural and human systems. Yet, the data in this report show that 2019 was already 1.1 °C warmer than the pre-industrial era. The consequences are already apparent. More severe and frequent floods, droughts and tropical storms, dangerous heatwaves and rising sea levels are already severely threatening lives and livelihoods across the planet.

We are currently way off track to meeting either the 1.5 °C or 2 °C targets that the Paris Agreement calls for. We need to reduce greenhouse gas emissions by 45% from 2010 levels by 2030 and reach net zero emissions by 2050. And for that, we need political will and urgent action to set a different path.

This report outlines the latest science and illustrates the urgency for far-reaching climate action. It brings together data from across the fields of climate science and lists the potential future impacts of climate change – from health and economic consequences to decreased food security and increased displacement.

I call on everyone – from government, civil society and business leaders to individual citizens – to heed these facts and take urgent action to halt the worst effects of climate change. We need more ambition on mitigation, adaptation and finance in time for the climate conference (COP26) to be held in Glasgow in November. That is the only way to ensure a safer, more prosperous and sustainable future for all people on a healthy planet.

(A. Guterres)
United Nations Secretary-General

Key messages

The global mean temperature for 2019 was 1.1±0.1 °C above pre-industrial levels. The year 2019 is likely to have been the second warmest in instrumental records. The past five years are the five warmest on record, and the past decade, 2010–2019, is also the warmest on record. Since the 1980s, each successive decade has been warmer than any preceding one since 1850.

Global atmospheric mole fractions of greenhouse gases reached record levels in 2018 with carbon dioxide (CO_2) at 407.8±0.1 parts per million (ppm), methane (CH_4) at 1869±2 parts per billion (ppb) and nitrous oxide (N_2O) at 331.1±0.1 ppb. These values constitute, respectively, 147%, 259% and 123% of pre-industrial levels. Early indications show that the rise in all three – CO_2, CH_4 and N_2O – continued in 2019.

The year 2019 saw low sea-ice extent in both the Arctic and the Antarctic. The daily Arctic sea-ice extent minimum in September 2019 was the second lowest in the satellite record. In Antarctica, variability in recent years has been high with the long-term increase offset by a large drop in extent in late 2016. Extents have since remained low, and 2019 saw record-low extents in some months.

The ocean absorbs around 90% of the heat that is trapped in the Earth system by rising concentrations of greenhouse gases. Ocean heat content, which is a measure of this heat accumulation, reached record-high levels again in 2019.

Over the decade 2009–2018, the ocean absorbed around 23% of the annual CO_2 emissions, lessening the increase in atmospheric concentrations. However, CO_2 absorbed in sea water decreases its pH, a process called ocean acidification. Observations from open-ocean sources over the last 20 to 30 years show a clear decrease in average pH at a rate of 0.017–0.027 pH units per decade since the late 1980s.

As the ocean warms it expands and sea levels rise. This rise is further increased by the melting of ice on land, which then flows into the sea. Sea level has increased throughout the altimeter record, but recently sea level has risen at a higher rate due partly to increased melting of ice sheets in Greenland and Antarctica. In 2019, the global mean sea level reached its highest value since the beginning of the high-precision altimetry record (January 1993).

Global Climate Indicators

Global Climate Indicators describe the changing climate, providing a broad picture of climate change at a global level that goes beyond temperature. They provide important information for the domains most relevant to climate change, including the composition of the atmosphere, the energy changes that arise from the accumulation of greenhouse gases and other factors, and the responses of land, oceans and ice. Key Global Climate Indicators include global mean surface temperature, atmospheric greenhouse gas concentrations, ocean heat content, global sea level, ocean acidification, sea-ice extent and the mass balance of glaciers and ice sheets.

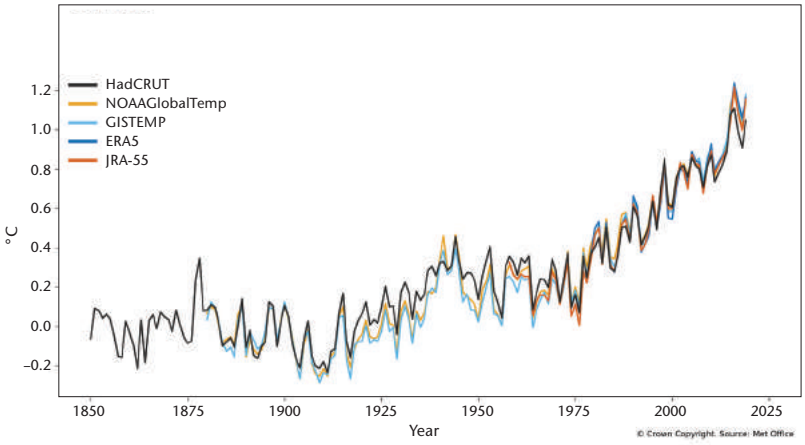

Figure 1. Global annual mean temperature difference from pre-industrial conditions (1850–1900). The two reanalyses (ERA5 and JRA-55) are aligned with the in situ datasets (HadCRUT, NOAAGlobalTemp and GISTEMP) over the period 1981–2010.

TEMPERATURE

The global mean temperature for 2019 was around 1.1 ± 0.1 °C above the 1850–1900 baseline, used as an approximation of pre-industrial levels. The year 2019 is likely to be the second warmest on record. The WMO assessment is based on five global temperature datasets[1] (Figure 1), with four of the five putting 2019 in second place and one dataset placing it third warmest. The spread of the five estimates is between 1.05 °C and 1.18 °C.

The Intergovernmental Panel on Climate Change (IPCC) *Special Report: Global Warming of 1.5 °C* (IPCC SR15) concluded that "Human-induced warming[2] reached approximately 1 °C (likely between 0.8 °C and 1.2 °C) above pre-industrial levels in 2017, increasing at 0.2 °C (likely between 0.1 °C and 0.3 °C) per decade (high confidence)". An update of the figures for 2019 is consistent with continued warming in the range of 0.1–0.3 °C per decade.

The year 2016, which began with an exceptionally strong El Niño, remains the warmest on record. Weak El Niño conditions in the first half of 2019 may have made a small contribution to the high global temperatures

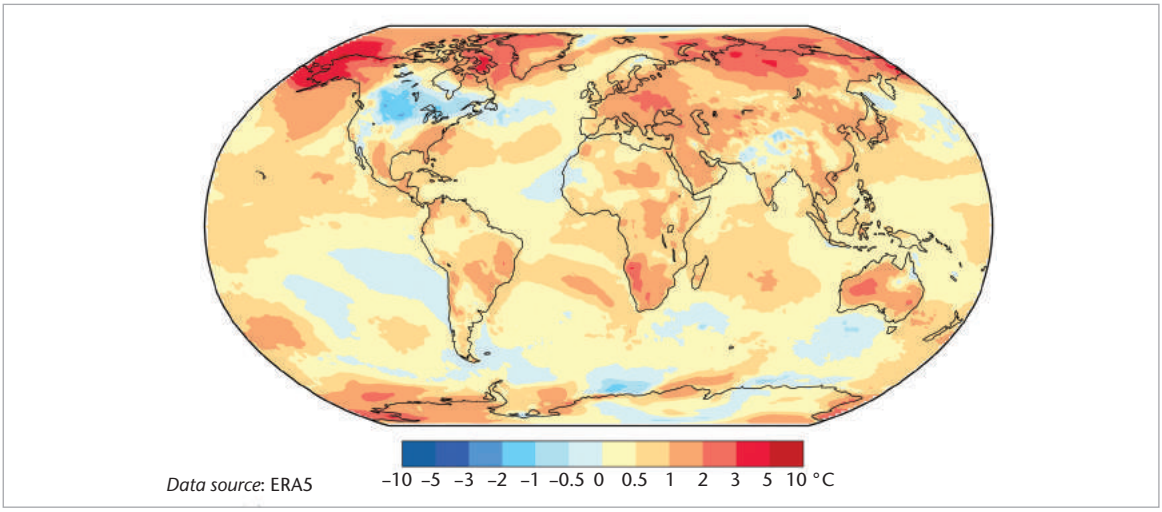

Figure 2. Surface-air temperature anomaly for 2019 with respect to the 1981–2010 average (*Source: European Centre for Medium-range Weather Forecasts (ECMWF) ERA5 data, Copernicus Climate Change Service*)

[1] The five datasets comprise three in situ datasets – HadCRUT.4.6.0.0 produced by the UK Met Office and the Climatic Research Unit at the University of East Anglia, NOAAGlobalTemp v5 produced by the US National Atmospheric and Oceanic Administration (NOAA), and GISTEMP v4 produced by the US National Aeronautics and Space Administration (NASA) Goddard Institute for Space Studies – as well as two reanalyses – ERA5 produced by the European Centre for Medium-range Weather Forecasts (ECMWF) for the Copernicus Climate Change Service, and JRA-55 produced by the Japan Meteorological Agency.

[2] Total warming refers to the actual temperature change, irrespective of cause, while human-induced warming refers to the component of that warming that is attributable to human activities. The estimate of human-induced warming is based on: Haustein, K. et al., 2017: A real-time Global Warming Index. *Scientific Reports* 7, 15417, doi:10.1038/s41598-017-14828-5.

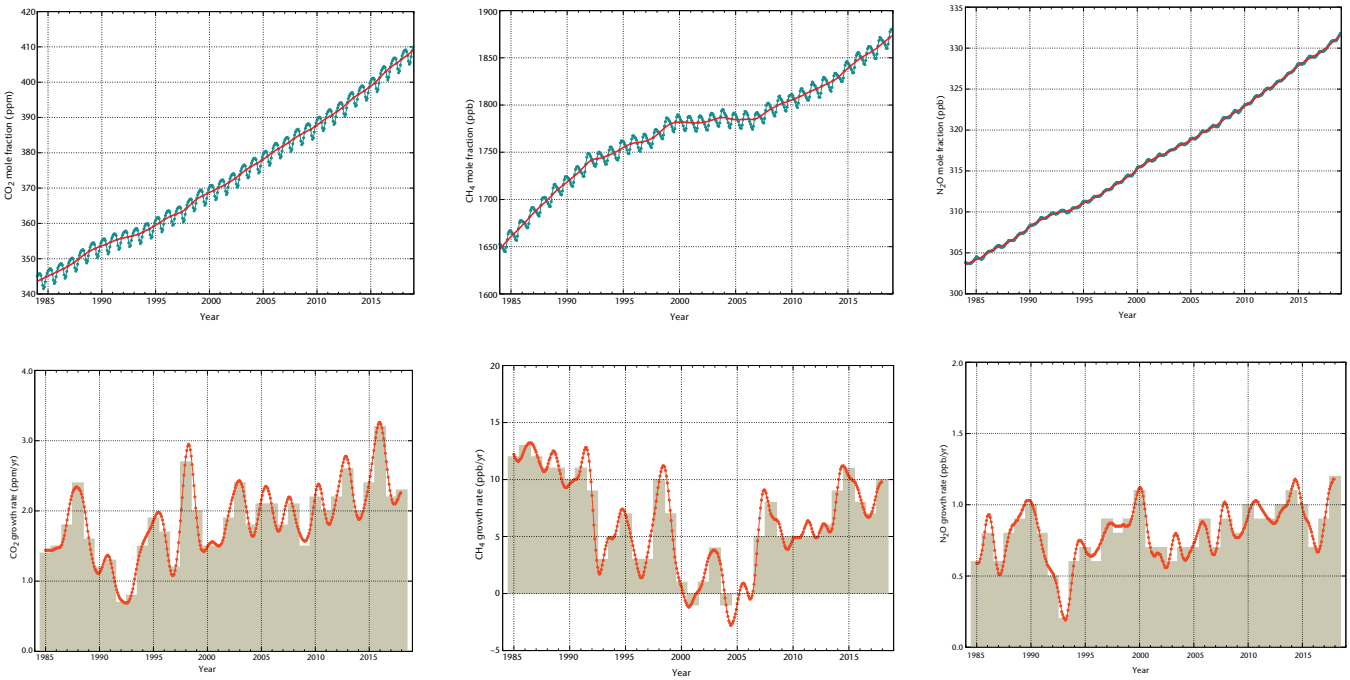

in 2019, but there was no clear increase in temperature at the start of the year as was seen in early 2016.

The past five years, 2015–2019, are the five warmest on record. The last five-year (2015–2019) and ten-year (2010–2019) averages are also the warmest on record.[3] Since the 1980s, each successive decade has been warmer than any preceding one since 1850.

Although the overall warmth of the year is clear, there were variations in temperature anomalies across the globe. Most land areas were warmer than the recent average (1981–2010, Figure 2). The year 2019 was among the top three warmest on record since at least 1950 over Africa. Other continental averages were among the three warmest, except the average for North America, which was nominally 14th warmest. The US State of Alaska was exceptionally warm. Areas of notable warmth for the year include large areas of the Arctic, central and eastern Europe, southern Africa, mainland south-east Asia, parts of Australia (where it was the warmest and the driest year on record), north-east Asia and parts of Brazil. Outside of North America, there were limited areas of below-average temperature over land.

GREENHOUSE GASES AND OZONE

Global averaged mole fractions of greenhouse gases are calculated from in situ observations at multiple sites, obtained through the Global Atmosphere Watch (GAW) Programme of WMO. These data are available from the World Data Centre for Greenhouse Gases operated by the Japan Meteorological Agency.[4] The year 1750 is used as a representative baseline for pre-industrial conditions.

Increasing levels of greenhouse gases in the atmosphere are a major driver of climate change. Atmospheric concentrations reflect a balance between sources (including emissions) and sinks. Global CO_2 concentrations reflect the balance between emissions due to human activities and uptake by the biosphere and ocean.

In 2018, greenhouse gas mole fractions reached new highs, with globally averaged mole fractions of CO_2 at 407.8±0.1 ppm, CH_4 at 1869±2 ppb and N_2O at 331.1±0.1 ppb (Figure 3). The annual increases in the three main greenhouse gases were larger than the increases in the previous year and the 10-year averaged growth rates. The global averaged mole fractions in 2018 constitute, respectively, 147%, 259% and 123% of pre-industrial (1750) levels.

Figure 3. Top row: Globally averaged mole fraction (measure of concentration), from 1984 to 2018, of CO_2 in parts per million (left), CH_4 in parts per billion (centre) and N_2O in parts per billion (right). The red line is the monthly mean mole fraction with the seasonal variations removed; the blue dots and line show the monthly averages. Bottom row: The growth rates representing increases in successive annual means of mole fractions for CO_2 in parts per million per year (left), CH_4 in parts per billion per year (centre) and N_2O in parts per billion per year (right) (*Source: WMO Global Atmosphere Watch*).

[3] For non-overlapping five- and ten-year periods.

[4] https://gaw.kishou.go.jp/

Global average figures for 2019 will not be available until late 2020, but real-time data from specific locations, including Mauna Loa (Hawaii) and Cape Grim (Tasmania) indicate that levels of CO_2, CH_4 and N_2O continued to increase in 2019.

The IPCC SR15 report found that limiting warming to 1.5 °C above pre-industrial levels implies reaching net zero CO_2 emissions globally around 2050 and concurrent deep reductions in emissions of non-CO_2 forcers, particularly methane.

CARBON BUDGET

Accurate assessment of anthropogenic CO_2 emissions and their redistribution among the atmosphere, ocean and terrestrial biosphere – the "global carbon budget"[5] – is important to better understand the global carbon cycle, support the development of climate policies, and project future climate change.

Fossil CO_2 emissions have increased steadily over the past two centuries, with brief interruptions due to minor falls associated with major economic downturns such as recessions or oil price shocks. Over the 2009–2018 decade, for which complete data are available, global fossil CO_2 emissions were on average 34.7 ± 1.8 $GtCO_2$ (billions of tonnes) per year, growing at an average rate of 0.9% per year to reach a record 36.6 $GtCO_2$ in 2018. Carbon dioxide emissions from land use change were 5.5 ± 2.6 $GtCO_2$ for the same period with no clear trend (Figure 4).

In the 2009–2018 decade, both atmospheric CO_2 concentration and its growth rate increased, and land and ocean CO_2 sinks continued to grow in response to the rise in atmospheric CO_2 concentrations. The land and ocean CO_2 sinks remove about 45% of all anthropogenic CO_2 emissions.

A preliminary projection of global fossil CO_2 emissions, using data from the first three quarters of 2019, suggested that emissions would grow 0.6% in 2019, with a range of -0.2% to +1.5% that includes the possibility of no growth or even slight decline in emissions relative to 2018. Fire emissions in deforestation zones indicate that emissions from land use change for 2019 were above the 2009–2018 average. In 2019, the growth rate in atmospheric CO_2 was 19.1 ± 3.3 $GtCO_2$, above the 2009–2018 average, with the increase driven by rising CO_2 emissions. The preliminary estimates for the ocean and land CO_2 sink in 2019 were 9.5 $GtCO_2$ and 14.3 $GtCO_2$ respectively, both above their decadal average.

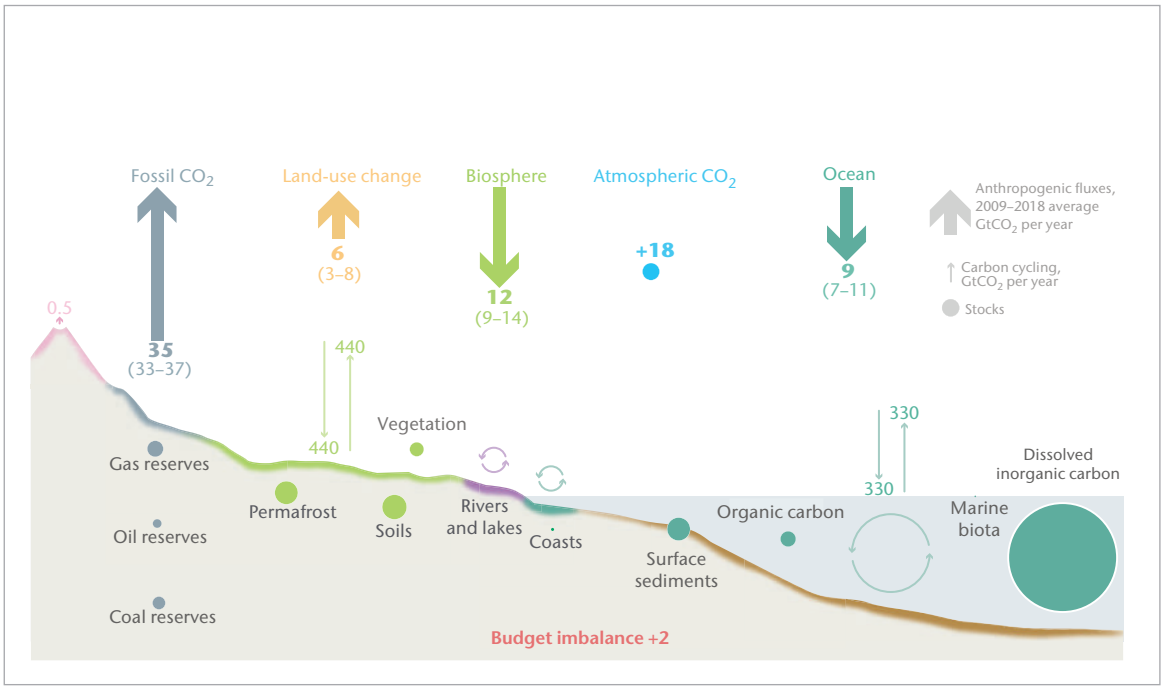

Figure 4. Perturbation budget of the global carbon cycle as a result of human activities, averaged globally for the decade 2009–2018. The anthropogenic perturbation occurs on top of natural carbon fluxes, with fluxes and stocks represented by thinner arrows and circles. The imbalance between total emissions and total sinks reflects the gaps in data, modelling or our understanding of the carbon cycle *(Sources: Global Carbon Project, http://www.globalcarbonproject.org/carbonbudget; Friedlingstein et al. 2019).*

[5] Friedlingstein, P. et al., 2019: Global Carbon Budget 2019. *Earth System Science Data*, 11, 1783–1838, https://www.earth-syst-sci-data.net/11/1783/2019/.

STRATOSPHERIC OZONE AND OZONE DEPLETING GASES

Following the success of the Montreal Protocol, the use of halons and chlorofluorocarbons (CFCs) has been reported as discontinued. Their levels in the atmosphere are monitored to understand the continued effect they have on the ozone layer and to detect unexpected changes. Recent studies reported a slowdown in the decline of the atmospheric concentration of CFC-11 after 2012,[6] connecting it to an increase in global emissions to which emissions from eastern Asia contributed. Because of their long atmospheric lifetime, these compounds will remain in the atmosphere for many decades. Even if there were no new emissions, there is more than enough chlorine and bromine present in the atmosphere to cause complete destruction of ozone at certain altitudes in Antarctica from August to December. Consequently, the formation of the ozone hole continues to be an annual spring event with year to year variation in its size and depth largely governed by meteorological conditions.

The 2019 ozone hole developed relatively early and continued growing until a sudden stratospheric warming in September disturbed the progression of the ozone destruction and led to the ozone hole being smaller and weaker than the long-term mean. The area of ozone depletion was below the long-term mean and the minimum ozone remained above the long-term mean until the beginning of November, several weeks earlier than usual. The ozone hole area reached its maximum for 2019 on 8 September, with 16.4 million km^2. By way of comparison, it reached 29.9 million km^2 on 9 September 2000 and 29.6 million km^2 on 24 September 2006, according to an analysis from the US National Aeronautics and Space Administration (NASA) (Figure 5).

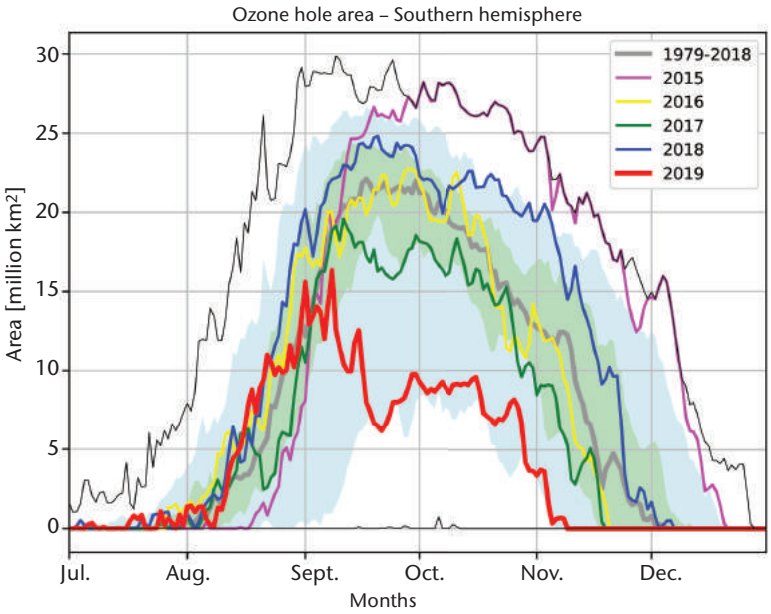

Figure 5. Area (millions of km^2) where the total ozone column is less than 220 Dobson units; 2019 is shown in red. The most recent years are shown for comparison as indicated by the legend. The smooth, thick grey line is the 1979–2018 average. The blue shaded area represents the 30th to 70th percentiles, and the green shaded area represents the 10th and 90th percentiles for the period 1979–2018. The thin black lines show the maximum and minimum values for each day in the 1979–2018 period. The plot is made at WMO on the basis of data downloaded from the NASA Ozone Watch (https://ozonewatch.gsfc.nasa.gov/). The NASA data are based on satellite observations from the OMI and TOMS instruments.

OCEAN

The ocean is an important part of the Earth system. The rate of change in ocean heat content is a measure of global warming, as it represents a large proportion of the heat accumulating in the climate system. Thermal expansion from ocean warming, combined with melting of ice on land, leads to sea level rise, which affects coastal areas. Changes in ocean chemistry associated with rising CO_2 concentrations in the atmosphere are altering the pH of the oceans.

OCEAN HEAT CONTENT

Ocean heat content (OHC) is a fundamental metric for climate change as it is a measure of heat accumulation in the Earth system. Human-induced atmospheric composition changes cause a radiative imbalance at the top of the atmosphere – Earth's energy imbalance – which is driving global warming.[7] Due to the ocean's large heat capacity, the majority (~90%) of this accumulated heat is stored in the global ocean.

Consequently, the ocean is warming, with wide-reaching impacts on the Earth climate system. For example, OHC increase contributes more than 30% of observed global mean sea-level rise through thermal expansion of sea water.[8] Ocean warming is altering ocean currents[9,10] and indirectly altering storm

[6] Montzka, S. A. et al., 2018: An unexpected and persistent increase in global emissions of ozone-depleting CFC 11. *Nature*, 557:413–417, doi:10.1038/s41586-018-0106-2.

[7] Hansen, J.et al., 2011: Earth's energy imbalance and implications. *Atmospheric Chemistry and Physics*, 11, 13 421–13 449.

[8] World Climate Research Programme (WCRP) Global Sea Level Budget Group, 2018: Global sea-level budget 1993–present. *Earth System Science Data*, 10, 1551–1590, https://doi.org/10.5194/essd-10-1551-2018.

[9] Hoegh-Guldberg, O. et al., 2018: Impacts of 1.5 °C Global Warming on Natural and Human Systems. In: Intergovernmental Panel on Climate Change (IPCC), 2018: *Global Warming of 1.5 °C* (Masson-Delmotte, V., P. Zhai, H.-O. Pörtner, D. Roberts, J. Skea, P.R. Shukla, A. Pirani, W. Moufouma-Okia, C. Péan, R. Pidcock, S. Connors, J.B.R. Matthews, Y. Chen, X. Zhou, M.I. Gomis, E. Lonnoy, T. Maycock, M. Tignor, and T. Waterfield, eds.). Geneva.

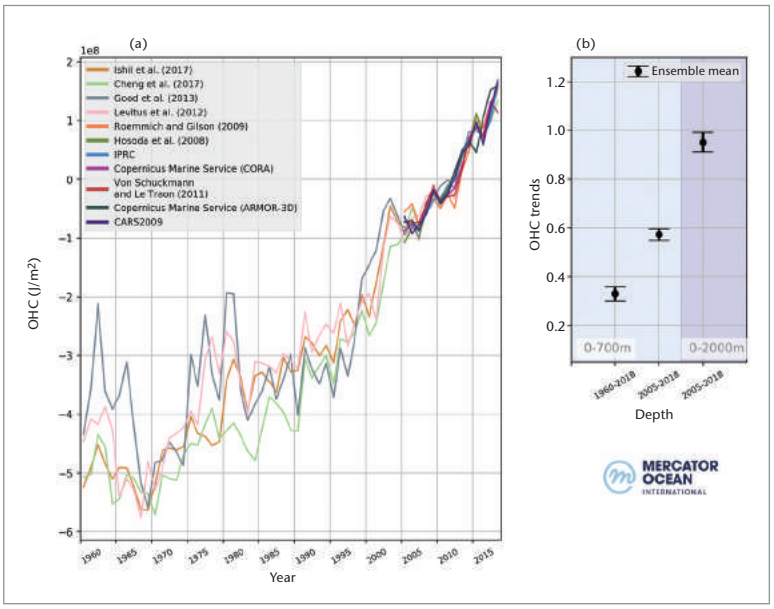

Figure 6. (a) Near-global (60° S–60° N) area averaged OHC over the period 1960–2018 and as derived from different subsurface temperature products. Argo-based products have been superimposed from the year 2005 onwards as indicated in the legend;[22] (b) Rate of change of the ensemble mean of OHC time series shown in (a), together with its ensemble spread. Rates amount to 0.3±0.1 Wm^{-2} (0–700 m, 1960–2018), 0.6±0.1 Wm^{-2} (0–700 m, 2005–2018), 1.0±0.1 Wm^{-2} (0–2000 m, 2005–2018).

tracks.[11,12] The implications of ocean warming are widespread across Earth's cryosphere too, as floating ice shelves become thinner and ice sheets retreat.[13,14,15,16] Ocean warming increases ocean stratification and, together with ocean acidification and deoxygenation, can lead to dramatic changes in ecosystem assemblages and biodiversity, to population extinction, coral bleaching, infectious diseases, changes in behaviour (including reproduction) and redistribution of habitats.[17,18,19]

Historical measurements back to the 1940s mostly relied on shipboard techniques, which constrained the availability of subsurface temperature observations at global scale and at depth.[20] Global-scale estimates of OHC are thus often limited to the period from 1960 onwards, and to a vertical integration from the surface down to a depth of 700 m. With the deployment of the Argo network of autonomous profiling floats, which reached target coverage in 2006, it is now possible to routinely measure OHC changes down to a depth of 2000 m[21] (Figure 6).

In 2019, OHC in the upper 700 m (a series of measurements starting in the 1950s) and in the upper 2000 m (a series of measurements starting in 2006) continued to rise reaching record or near-record levels, with the average for the year exceeding the previous record highs set in 2018. In the last quarter of the decade and compared to the historical heat uptake since 1960, global ocean heat gain has increased in the upper (0–700 m) layer, and heat has been sequestered in the deeper ocean layers (0–2000 m).

[10] Rhein, M.et al., 2018: Greenland submarine meltwater observed in the Labrador and Irminger Seas. *Geophysical Research Letters*, 45, https://doi.org/10.1029/2018GL079110.

[11] Yang, H. et al., 2016: Intensification and poleward shift of subtropical western boundary currents in a warming climate. *Journal of Geophysical Research: Oceans*, 121, 4928–4945, doi:10.1002/2015JC011513.

[12] Woollings, T. et al., 2012: Response of the North Atlantic storm track to climate change shaped by ocean - atmosphere coupling. *Nature Geoscience*, May 2012, doi: 10.1038/NGEO1438.

[13] Shi, J. R. et al., 2018: Evolving relative importance of the Southern Ocean and North Atlantic in anthropogenic ocean heat uptake. *Journal of Climate*, 31, 7459--7479, https://doi.org/10.1175/JCLI-D-18-0170.1.

[14] Polyakov, I. V. et al., 2017: Greater role for Atlantic inflows on sea-ice loss in the Eurasian basin of the Arctic ocean. *Science*, 356, 285-291, doi: 10.1126/science.aai8204.

[15] Straneo, F. et al., 2019: The case for a sustained Greenland Ice sheet - Ocean Observing System (GrIOOS). *Frontiers in Marine Science*, 6, 138, doi: 10.3389/fmars.2019.00138.

[16] Shepherd, A. et al., 2018: Trends and connections across the Antarctic cryosphere. *Nature*, 558(7709), pp. 223-232, https://doi.org/10.1038/s41586-018-0171-6.

[17] Gattuso, J-P. et al., 2015: Contrasting futures for ocean and society from different anthropogenic CO_2 emissions scenarios. *Science*, 349, 6243, doi: 10.1126/science.aac4722.

[18] Molinos, J.G. et al., 2016: Climate velocity and the future global redistribution of marine biodiversity. *Nature Climate Change*, 6, https://doi.org/10.1038/nclimate2769.

[19] Ramírez, F. et al., 2017: Climate impacts on global hot spots of marine biodiversity. *Science Advances*, 3(2), doi: 10.1126/sciadv.1601198.

[20] Abraham, J. P. et al., 2013: A review of global ocean temperature observations: implications for ocean heat content estimates and climate change. *Review of Geophysics*, 51, 450–483, doi: 10.1002/rog.20022.

[21] Riser, S. et al., 2016: Fifteen years of ocean observations with the global Argo array. *Nature Climate Change*, 6, 145–153, https://doi.org/10.1038/nclimate2872.

[22] More information on the different data products used can be found in the references mentioned in the legend; for CARS2009, further information is available at http://www.marine.csiro.au/~dunn/cars2009/), for the International Pacific Research Centre (IPRC) at http://apdrc.soest.hawaii.edu/projects/argo/, and for the Copernicus Marine Service at http://marine.copernicus.eu/.

MARINE HEATWAVES

As with heatwaves on land, extreme heat can affect the near-surface layer of the oceans with a range of consequences for marine life and dependent communities. Satellite retrievals of sea-surface temperature can be used to monitor marine heatwaves (MHWs). In this case, MHWs are categorized as follows: moderate, when the sea-surface temperature is above the 90th percentile of the climatological distribution for five days or longer;[23] strong, if the difference from the long-term average is more than twice that between the 90th percentile and the long-term mean; severe, if the difference from the long-term average is more than three times as large, and extreme, if that difference is more than four times as large.

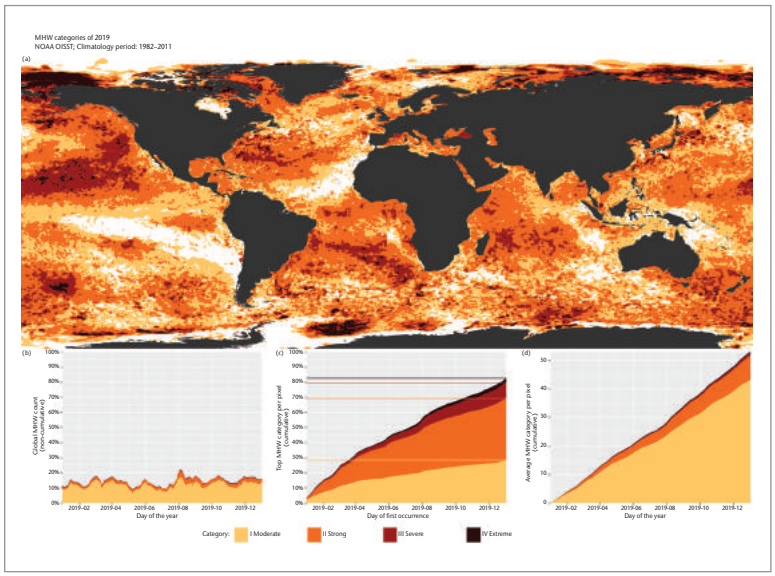

Figure 7. (a) Global map showing the highest MHW category experienced at each pixel over the course of the year, estimated using the NOAA OISST v2 dataset (reference period 1982–2011). White indicates that no MHWs occurred in a pixel over the entire year; (b) Stacked bar plot showing the percentage of ocean pixels experiencing an MHW on any given day of the year; (c) Stacked bar plot showing the cumulative percentage of the ocean that experienced an MHW over the year.[29] Horizontal lines in this figure show the final percentages for each category of MHW; (d) Stacked bar plot showing the cumulative number of MHW days averaged over all pixels in the ocean[30] *(Source: Robert Schlegel, Woods Hole).*

For 2019 (Figure 7), the number of MHW days averaged over the entire ocean was approximately 55 days per pixel, nearly 2 months of unusually warm temperatures. More of the ocean had an MHW classified as strong (41%) rather than moderate (29%), and 84% of the ocean experienced at least one MHW. In large areas of the north-east Pacific, MHWs reached the "severe" category. From 2014 to 2016, sea-surface temperatures in the area were also unusually high and the mass of warmer than average waters was dubbed the "blob".[24,25] Another notable area is the Tasman Sea, where there has been a series of MHWs in the summers of 2015/2016,[26] 2017/2018[27] and again in 2018/2019. In late 2019, an extreme MHW also affected the area to the east of New Zealand. Climate events, including MHWs and floods, were associated with extensive mortality of key marine habitat-forming communities along more than 45% of Australia's continental coastline, between 2011 and 2017.[28]

SEA LEVEL

In 2019, the sea level continued to rise (Figure 8, left), with the global mean sea level reaching its highest value since the beginning of the high-precision altimetry record (January 1993). The average rate of rise is estimated at 3.24 ± 0.3 mm yr^{-1} over the 27 year period, but the rate has increased over that time. A greater loss of ice mass from the ice sheets is the main cause of the accelerated rise in the global mean sea level[8] on top of steady increases from the expansion of ocean waters driven by warming.

---

[23] Hobday, A.J. et al., 2018 : Categorizing and naming marine heatwaves. *Oceanography* 31(2), https://doi.org/10.5670/oceanog.2018.205.

[24] Gentemann, C. L. et al., 2017: Satellite sea surface temperatures along the West Coast of the United States during the 2014–2016 northeast Pacific marine heat wave. *Geophysical Research Letters*, 44, 312– 319, doi:10.1002/2016GL071039.

[25] Di Lorenzo, E. and N. Mantua, 2016: Multi-year persistence of the 2014/15 North Pacific marine heatwave. *Nature Climate Change*, 6(11), p.1042, doi: 10.1038/nclimate308.

[26] Oliver, E.C. et al., 2017. The unprecedented 2015/16 Tasman Sea marine heatwave. *Nature communications*, 8, p.16101, doi: 10.1038/ncomms16101.

[27] Perkins-Kirkpatrick, S.E. et al., 2019: The role of natural variability and anthropogenic climate change in the 2017/18 Tasman Sea marine heatwave. *Bulletin of the American Meteorological Society*, 100(1), pp.S105-S110, https://doi.org/10.1175/BAMS-D-18-0116.1.

[28] Babcock, R. C. et al., 2019: Severe continental-scale impacts of climate change are happening now: Extreme climate events impact marine habitat forming communities along 45% of Australia's coast. *Frontiers in Marine Science*, 6, https://doi.org/10.3389/fmars.2019.00411.

[29] These values are based on when in the year a pixel first experiences its highest MHW category, so no pixel is counted more than once.

[30] This is taken by finding the cumulative MHW days per pixel for the entire ocean and dividing that by the overall number of ocean pixels (~690 000).

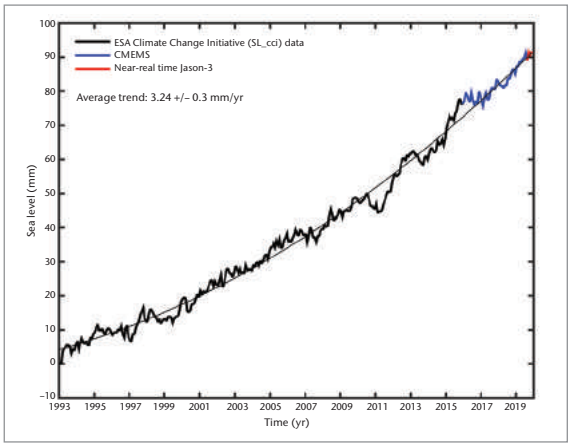

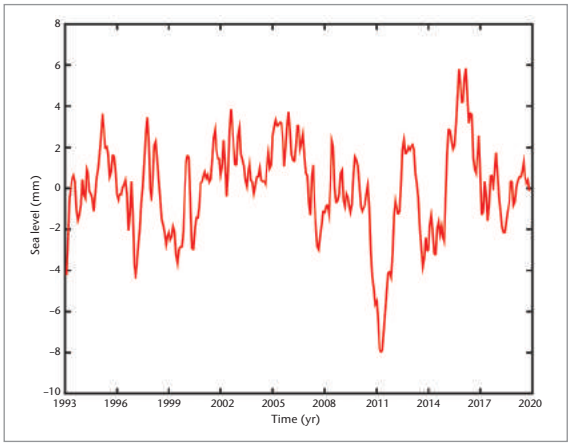

Figure 8. Left: Global mean sea-level evolution for January 1993–December 2019, from high-precision altimetry. The thin black curve is a quadratic function that best fits the data. The data from the Copernicus Marine Environment Monitoring Service (CMEMS) begin in January 2016 and those from the European Organization for the Exploitation of Meteorological Satellites (EUMETSAT) Jason-3 in October 2019. Right: Detrended global mean sea level over the same period (the difference between the smooth quadratic function and the measured values in the left panel).

Interannual variability (Figure 8, right) in sea-level rise is mainly driven by the El Niño-Southern Oscillation (ENSO, see also the section Drivers of short-term climate variability). During El Niño, water from tropical river basins on land is transferred to the ocean by shifts in precipitation and run-off (as was the case in 1997, 2012 and 2015). During La Niña, the opposite occurs, with a transfer of water from the ocean to land (for example, in 2011).[31]

Sea-level rise is not regionally uniform. Figure 9 shows the spatial trend patterns from January 1993 to May 2019. The strongest regional trends in the southern hemisphere are east of Madagascar in the Indian Ocean, east of New Zealand in the Pacific Ocean, and east of Rio de la Plata/South America in the South Atlantic. In the northern hemisphere, an eastward, elongated pattern is also seen in the North Pacific. A previously strong pattern seen in the western tropical Pacific over the first two decades of the altimetry record is now fading, suggesting that it was not a long-term signal. Non-uniform sea-level trends are dominated by geographical variations in OHC[32,33] but also depend on processes involving the atmosphere, geosphere and cryosphere.

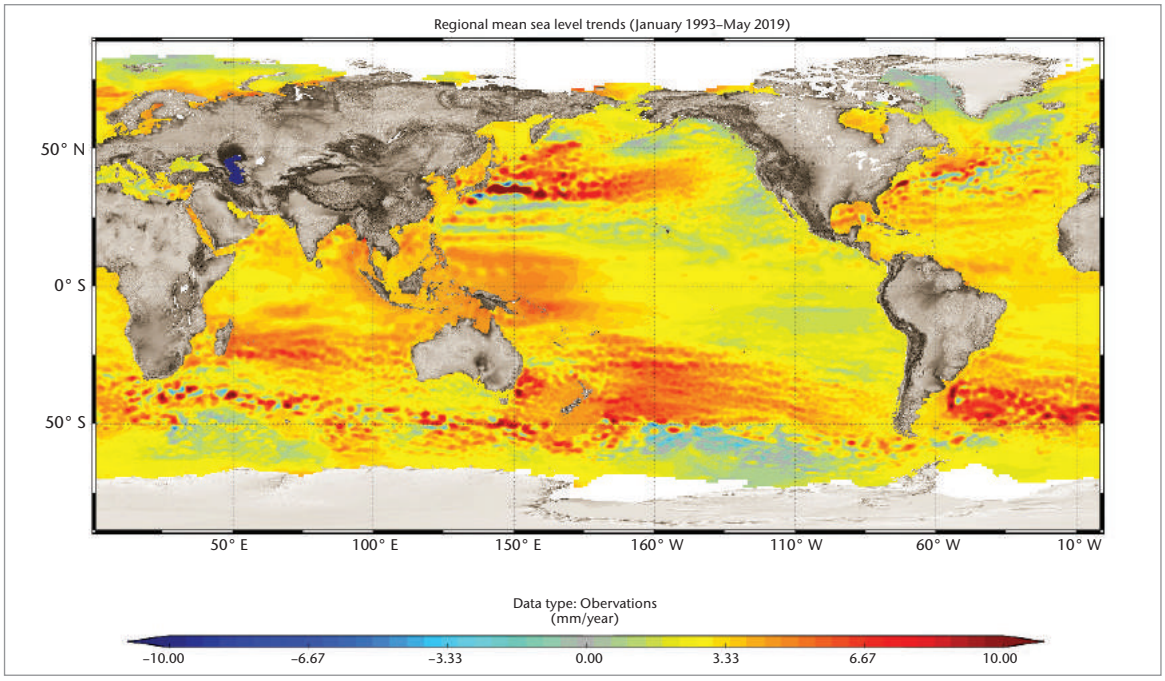

Figure 9. Regional variability in sea-level trends 1993–2019 based on satellite altimetry *(Source: Copernicus/ Collecte Localisation Satellites (CLS)/Centre national d'études spatiales (CNES)/ Laboratoire d'Études en Géophysique et Océanographie Spatiales (LEGOS)).*

[31] Fasullo, J. T. et al., 2013: Australia's unique influence on global sea level in 2010–2011. *Geophysical Research Letters*, 40, 4368–4373, doi:10.1002/grl.50834.

[32] Church, J. A. et al., 2013: Sea Level Change. In: Intergovernmental Panel on Climate Change (IPCC), 2013: *Climate Change 2013: The Physical Science Basis*. Contribution of Working Group I to the Fifth Assessment Report of the Intergovernmental Panel on Climate Change (Stocker, T. F. et al. (eds.)]. Cambridge and New York, Cambridge University Press.

OCEAN ACIDIFICATION

In the decade 2009–2018, the ocean absorbed around 23% of annual CO_2 emissions,[34] which helps to alleviate the impact of climate change. However, increasing atmospheric CO_2 concentrations alter the chemistry of the ocean as CO_2 reacts with seawater decreasing its pH and increasing the acidity of the ocean. This process is called ocean acidification. The change in pH is linked to other shifts in carbonate chemistry that decrease the ability of some marine organisms – such as mussels, crustacean and corals – to calcify. The combined changes affect marine life, lessening the potential for growth and reproduction. Observations from open-ocean sources over the last 20 to 30 years show a clear decrease in average pH, with a decline of the average global surface ocean pH of 0.017–0.027 pH units per decade since the late 1980s.

In coastal seas, changes in carbonate chemistry caused by anthropogenic ocean acidification are more difficult to distinguish, due to the complexity of the environment and the variety of influences on it. These changes affect ocean services that are centred on the coast, which are important for human well-being, such as fisheries and aquaculture, tourism and recreation. Strong seasonal patterns and variability in pH are evident in recent monitoring efforts in the Southern Ocean around New Zealand (Figure 10), highlighting the need for sustained long-term observations with high temporal and spatial resolution.

DEOXYGENATION

Both observations and numerical models indicate that oxygen is declining in the modern open and coastal oceans, including estuaries and semi-enclosed seas. Since the middle of the last century, there has been an estimated 1%–2% decrease (that is, 2.4–4.8 Pmol or 77 billion–145 billion tons) in the global ocean oxygen inventory.[35,36] However, ocean observations at 200-m depths show

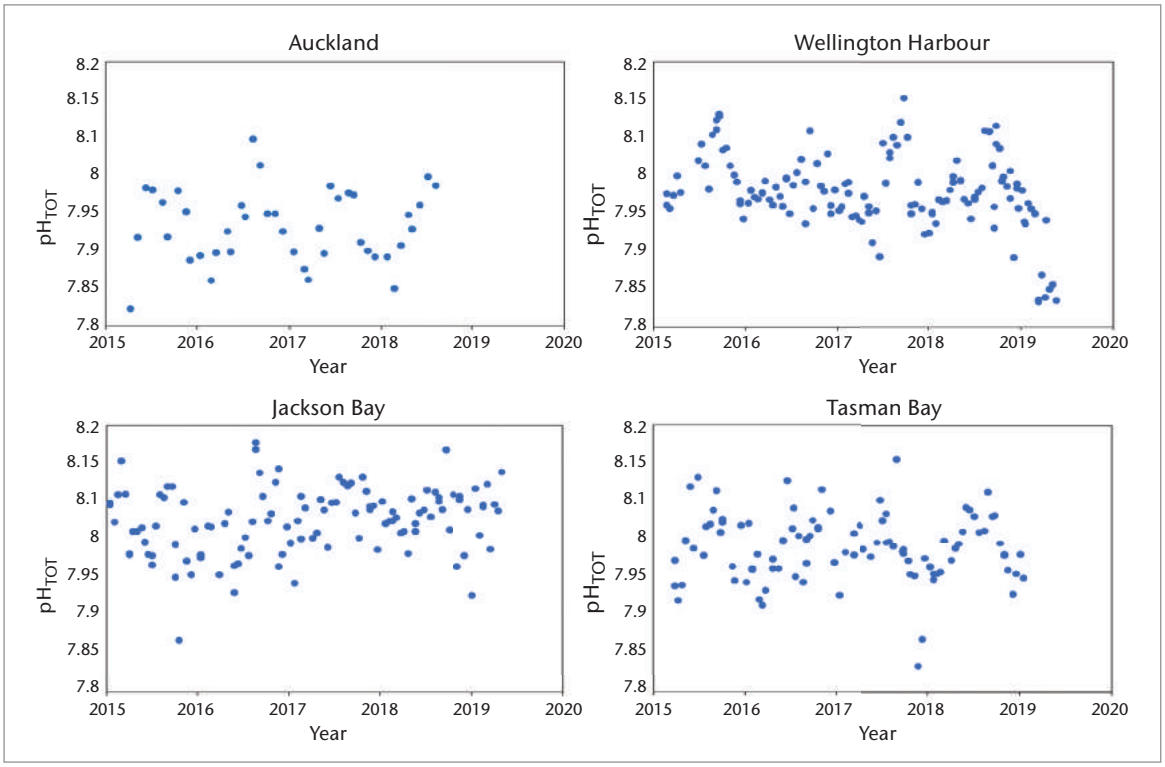

Figure 10. Measurements of pH from four sites around New Zealand, spanning four to five years of observations. Top row: Urbanized sites in Auckland and Wellington. Bottom row: One open coast (Jackson Bay) and one bay (Tasman Bay) site. Seasonal patterns and variability between pH measurements are clearly visible *(Credit: Kim Currie, National Institute of Water and Atmospheric Research (NIWA)).*

[33] Intergovernmental Panel on Climate Change (IPCC), 2019: *IPCC Special Report on the Ocean and Cryosphere in a Changing Climate* (H.-O. Pörtner, D.C. Roberts, V. Masson-Delmotte, P. Zhai, M. Tignor, E. Poloczanska, K. Mintenbeck, M. Nicolai, A. Okem, J. Petzold, B. Rama, N. Weyer (eds.)). In press.

[34] World Meteorological Organization (WMO), 2019: *WMO Greenhouse Gas Bulletin: The State of Greenhouse Gases in the Atmosphere. Based on Global Observations through 2018*, https://library.wmo.int/doc_num.php?explnum_id=10100.

[35] Bopp, L. et al., 2013: Multiple stressors of ocean ecosystems in the 21st century: Projections with CMIP5 models. *Biogeosciences*, 10:6225–6245, https://doi.org/10.5194/bg-10-6225-2013.

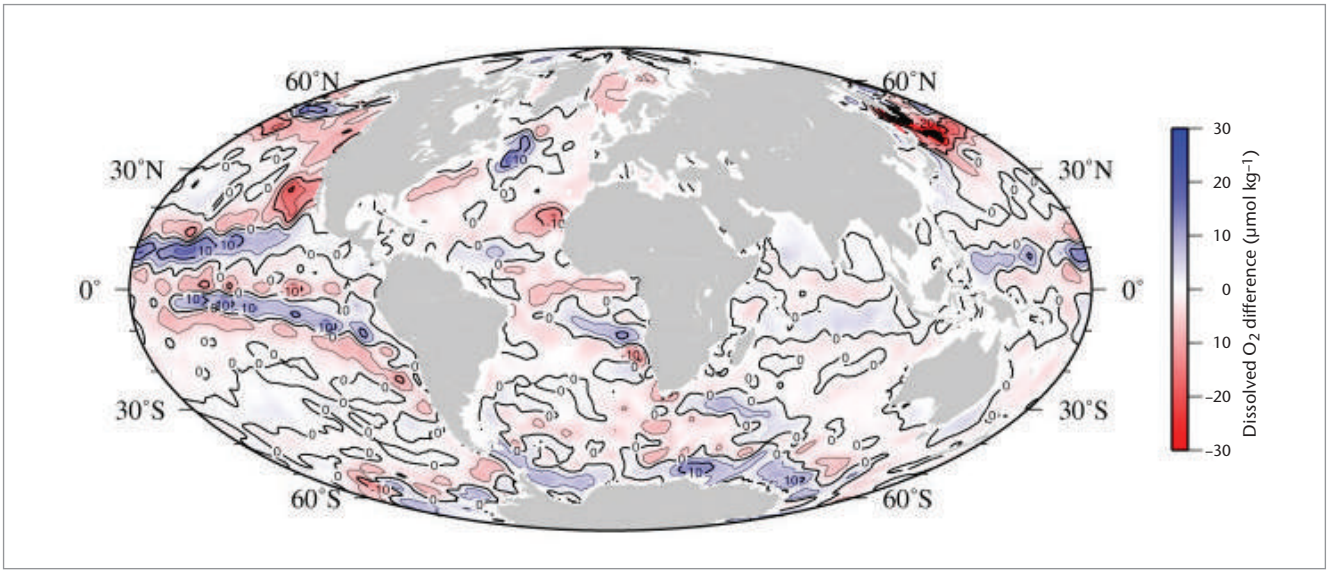

Figure 11. Dissolved oxygen difference between 2000–2018 and 1970–2018 using in situ measurements in 200-m seawater (bottle data), based on World Ocean Atlas 2018 (Garcia et al., 2018).

that changes vary across the ocean basins, with the highest loss of dissolved oxygen in the northern hemisphere in the last decades (Figure 11).

The projected 7% expansion of the pre-industrial area of oxygen minima (< 80 µmol kg^{-1}) by 2100 is expected to alter the diversity, composition, abundance and distribution of marine life. New studies further identified deoxygenation alongside ocean warming and ocean acidification as a major threat to ocean ecosystems and human well-being. Even coral reefs are now recognized as vulnerable to major oxygen loss.[37]

CRYOSPHERE

The cryosphere includes solid precipitation, snow cover, sea ice, lake and river ice, glaciers, ice caps, ice sheets, permafrost and seasonally-frozen ground. The cryosphere provides key indicators of a changing climate, yet it is one of the most under-sampled domains of the Earth system. Many of the components are measured at the surface, but spatial coverage is generally poor. Some, like sea ice extent, have been measured from space for many years, while the capability to measure other components from space is still developing. The major cryosphere indicators used here include sea-ice extent, glacier mass balance and the Greenland ice-sheet mass balance. Specific snow events are covered in the section High-impact events in 2019.

SEA ICE

Arctic (as well as sub-Arctic) sea ice has seen a long-term decline in all months during the satellite era (1979–present, Figure 12), with the largest relative losses in late summer, around the time of the annual minimum in September, with regional variations.

The 2019 Arctic winter maximum daily sea-ice extent (14.78 million km^2), reached around 13 March, was the 7th lowest maximum on record,[38] and the March monthly average was also the 7th lowest (Figure 12). The Arctic summer minimum daily sea-ice extent (4.15 million km^2), which occurred around 18 September, was tied with 2007 and 2016 as the second lowest on record.[39] The September

[36] Schmidtko, S. et al., 2017: Decline in global oceanic oxygen content during the past five decades. *Nature*, 542:335–339, doi: 10.1038/nature21399.

[37] Camp E.F. et al., 2017: Reef-building corals thrive within hot-acidified and deoxygenated waters. *Scientific Reports*, 7(1), 2434, doi: 10.1038/s41598-017-02383-y.

[38] http://nsidc.org/arcticseaicenews/2019/03/

[39] http://nsidc.org/arcticseaicenews/2019/09/

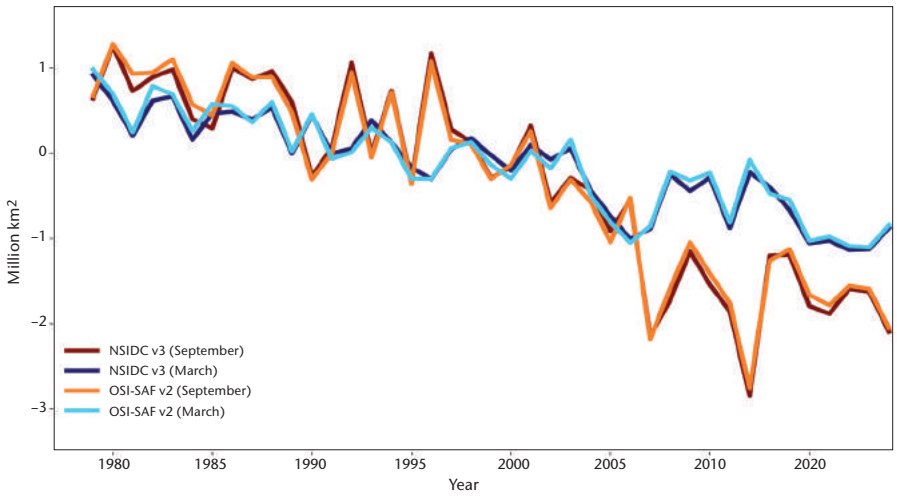

Figure 12. Monthly September and March Arctic sea-ice extent anomalies (relative to the 1981–2010 average) for 1979– 2019 *(Sources: US National Snow and Ice Data Center (NSIDC) and EUMETSAT Ocean and Sea Ice Satellite Application Facility (OSI SAF))*

monthly average extent was nominally the 3rd lowest on record.[40]

Extents remained very low till November, with the ice edge advancing more slowly than normal in the Beaufort, Chukchi, Kara and Barents Seas. Around Svalbard, however, the sea ice returned to near average conditions.[41] From April to November 2019, monthly extents were among the three lowest on record for those months, with the monthly extent for October being the lowest on record.

Ice conditions varied considerably during the 2018/2019 winter in the Arctic regional seas. Although ice extent was extremely low in the Bering Sea, it was close to normal in the adjacent Sea of Okhotsk. Northerly winds in the Barents Sea region, from January to August 2019, meant that ice extent was close to normal in the northern part of this area, unlike the past decade when it was lower than average. Winter 2018/2019 brought early ice formation on the Great Lakes of North America and above-average ice coverage. The maximum ice coverage on the Great Lakes was 145% of the long-term average and the 7th highest since 1972/1973.[42]

Until 2016, Antarctic sea-ice extent had shown a small long-term increase (Figure 13). In late 2016, this was interrupted by a sudden drop in extent to extremely low values. Since then, Antarctic sea-ice extent has remained at relatively low levels. The year 2019 saw three months with record-low monthly extents (May, June and July). Late austral winter and spring saw extents that were closer to the long-term average, but November had its 2nd lowest extent on record, and December its

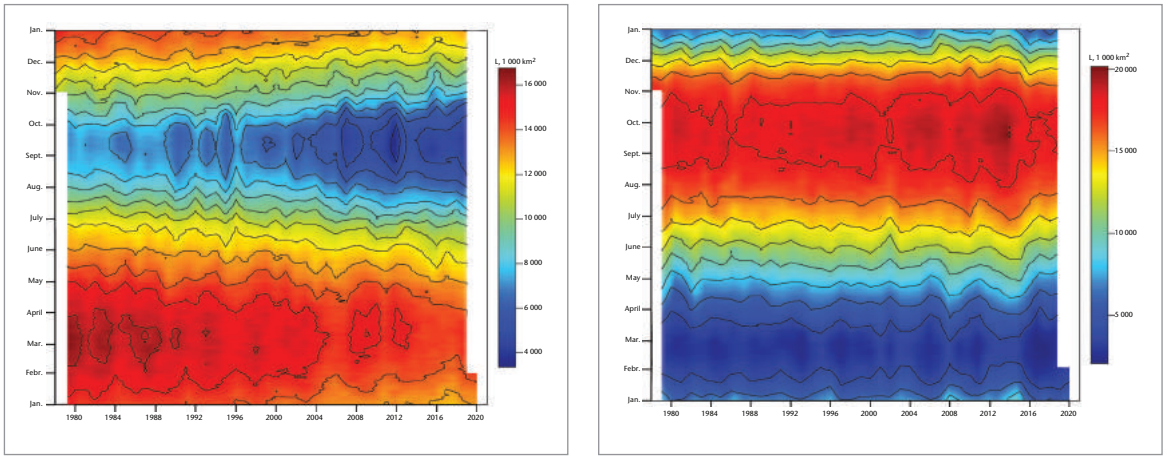

Figure 13. Variability of seasonal patterns of daily sea-ice extent for the Arctic (north of 45° N, left) and Antarctic (south of 50° S, right) calculated on the basis of the NSIDC NASA Team series for 1978–2020 *(Source: Arctic and Antarctic Research Institute (AARI))*

[40] http://nsidc.org/arcticseaicenews/2019/10/

[41] http://nsidc.org/arcticseaicenews/2019/11/

[42] https://www.glerl.noaa.gov/data/ice/#historical

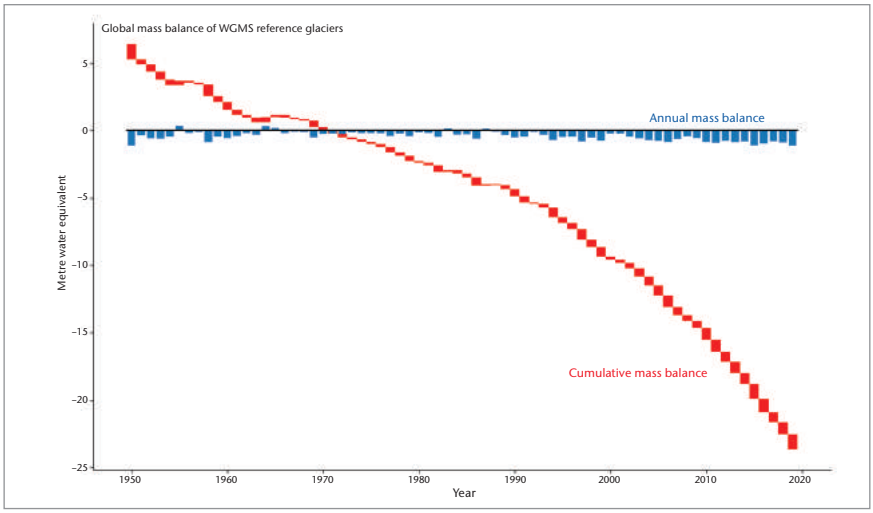

Figure 14. Annual (blue) and cumulative (red) mass balance of reference glaciers with more than 30 years of ongoing glaciological measurements. Global mass balance is based on an average for 19 regions to minimize bias towards well-sampled regions. Annual mass changes are expressed in meter water equivalent (m w.e.) which corresponds to tonnes per square meter (1 000 kg m^{-2}) *(Source: World Glacier Monitoring Service (WGMS, 2020, updated).*

4th or 5th lowest. The minimum daily sea-ice extent (2.47 million km^2), reached around 28 February, was the 7th lowest on record. The maximum daily sea-ice extent (18.40 million km^2) was reached around 30 September.

GLACIERS

Glaciers are formed from snow that has compacted to form ice, which can deform and flow downhill to lower, warmer altitudes, where it melts or, if the glacier terminates in the ocean, breaks up forming icebergs. Glaciers are sensitive to changes in temperature, precipitation and incoming solar radiation as well as other factors such as changes in basal lubrication or the loss of buttressing ice shelves.

According to the World Glacier Monitoring Service, in the hydrological year 2017/2018, observed glaciers experienced an ice loss of 0.89 metre water equivalent (m w.e.) (Figure 14). Preliminary results for 2019, based on a subset of glaciers, indicate that the hydrological year 2018/2019 was the thirty-second consecutive year of negative mass balance, with an ice loss in excess of 1 m w.e. Eight out of the ten most negative mass-balance years have been recorded since 2010. The cumulative loss of ice since 1970 amounts to over 23 m w.e.

The year 2019 saw major losses in ice volume from Swiss glaciers, as reported by the Cryospheric Commission of the Swiss Academy of Sciences,[43] though overall losses were lower than in the previous two years. In late spring, snow cover on the glaciers was around 20% to 40% above normal and, although the onset of melt was relatively late, the rate of loss reached record levels in late June and early July during a two-week period of intense heat. Melting continued until the beginning of September. In the 12 months to October 2019, around 2% of Switzerland's total glacier volume was lost. Over the past five years, the loss has exceeded 10%, the highest rate of decline in more than a century of records.

GREENLAND ICE SHEET

Changes in the mass of the Greenland ice sheet reflect the combined effects of surface mass balance (SMB) – defined as the difference between snowfall and run-off from the Greenland ice sheet, which is always positive at the end of the year – and mass losses at the periphery from the calving of icebergs and the melting of glacier tongues that meet the ocean.[44]

The total accumulated SMB between September 2018 and August 2019 (Figure 15, left) was 169 Gt, which is the 7th lowest on record. Nine of the 10 lowest SMB years since 1981 have been observed in the last 13 years. By way of comparison, the average SMB for 1981–2010 is 368 Gt, and the lowest SMB was 38 Gt in 2012. The surface mass balance was below normal almost everywhere in Greenland except the southeast (Figure 15,

[43] https://naturalsciences.ch/organisations/ekk/118503-glacier-volume-reduced-by-10-per-cent-in-only-five-years

[44] Based on the Polar Portal seasonal report for 2019 available at http://polarportal.dk/en/home/2019-season-report/.

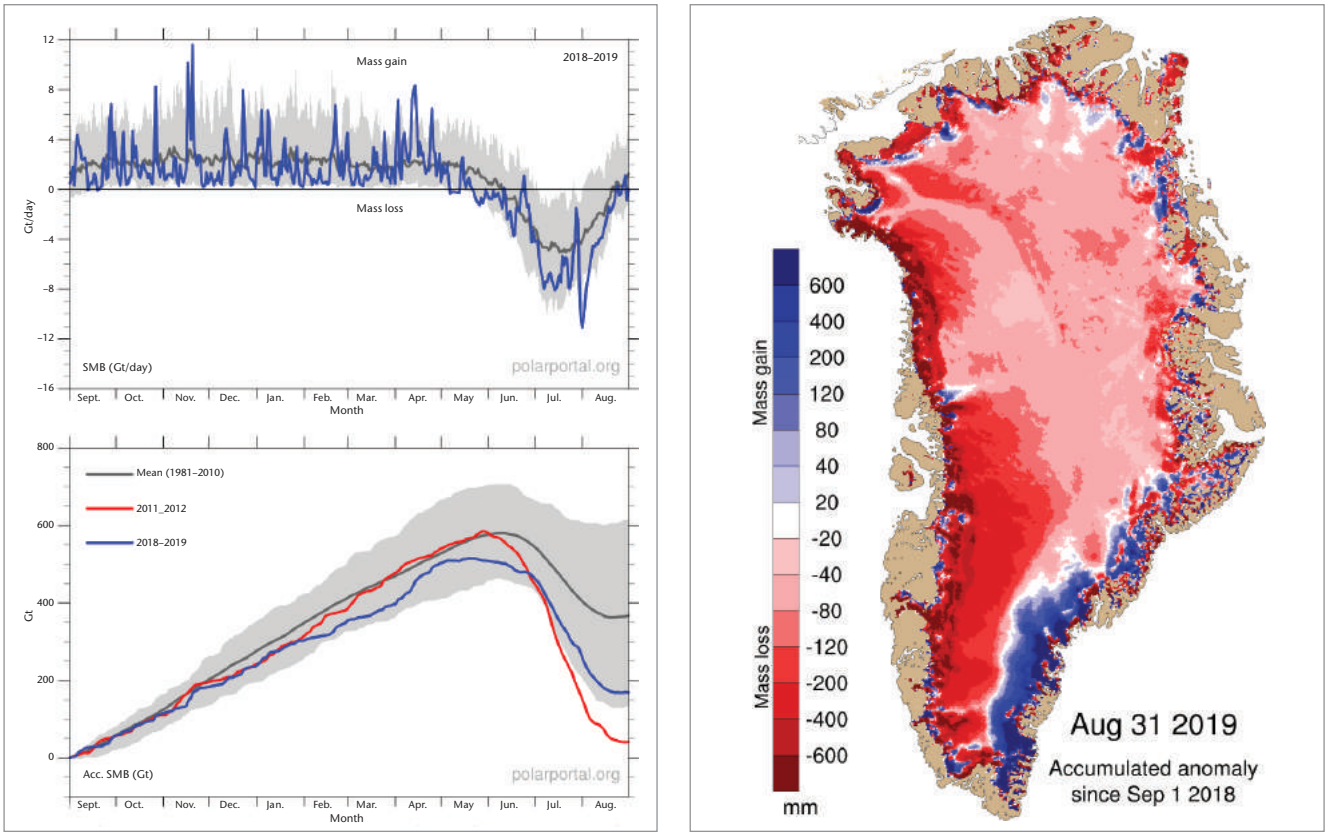

right). This was due to a dry winter, a very early start of the melting season and a long, dry, warm summer.

As noted earlier, SMB is always positive at the end of the year, but the ice sheet also loses ice through calving of icebergs and melting where the glacier tongues meet warm sea water. With satellites we can measure the ice velocity of the outlet glaciers around the edges of the ice sheet, and from that we can estimate how much ice is lost through calving and ocean melting. The analysis for 2018/2019 gives a loss of about 498 Gt. In comparison, the ice sheet lost an average of about 462 Gt per year as icebergs and through ocean melting over the period 1986–2018.

Combining a gain in SMB of 169 Gt with ice loss from calving and ocean melting of 498 Gt gives a net ice loss for 2018/2019 of 329 Gt. To put this in context, data from the Gravity Recovery and Climate Experiment (GRACE) satellites tell us that Greenland lost about 260 Gt of ice per year over the period 2002–2016, with a maximum of 458 Gt in 2011/2012. So, the 329 Gt of this season is well above the average, but not a record loss.

DRIVERS OF SHORT-TERM CLIMATE VARIABILITY

The ocean plays several important roles in the climate. Surface temperatures change relatively slowly over the ocean so recurring patterns in sea-surface temperature can be used to understand and, in some cases, predict the more rapidly changing patterns of weather over land on seasonal time scales. Two factors, in particular, that can help to understand the climate of 2019, are the El Niño-Southern Oscillation and the Indian Ocean Dipole.

EL NIÑO-SOUTHERN OSCILLATION

The El Niño-Southern Oscillation (ENSO) is one of the most important drivers of year-to-year variability in global weather patterns. El Niño events, characterized by warmer than average sea-surface temperatures in the eastern Pacific and a weakening of the trade winds, are associated with higher global temperatures. Cooler global temperatures often accompany La Niña events, which are characterized by cooler than average sea-surface temperatures in the eastern Pacific and a strengthening of the trade winds.

Figure 15. Left: SMB for the year 1 September 2018 to 31 August 2019. The upper panel shows individual days, and the lower panel the accumulated sum over the year. The year 2018/2019 is in blue, and the grey line is the long-term average. By way of comparison, the lower panel shows the record year 2011/2012 in red. Units are gigatonnes (Gt) per day and gigatonnes, respectively. Right: Map showing SMB anomaly (in mm) across Greenland *(Source: Polar Portal, http://polarportal.dk/en)*

Record global temperatures in 2016 followed an unusually strong El Niño event in late 2015 and early 2016. In contrast, 2019 started with neutral or weak El Niño conditions.[45] Sea-surface temperatures reached or exceeded typical El Niño thresholds from October 2018 through the first half of 2019, but an atmospheric response was absent in the early stages of the event. Atmospheric indicators such as weakened trade winds and increased cloudiness at the dateline did not show consistently until February. Thereafter, coupling between the ocean and the atmosphere maintained sea-surface temperatures at borderline El Niño levels until the middle of the year.

INDIAN OCEAN DIPOLE

The positive phase of the Indian Ocean Dipole (IOD) is characterized by cooler than average sea-surface temperatures in the eastern Indian Ocean and warmer than average sea-surface temperatures in the west. The negative phase has the opposite pattern. The resulting change in the gradient of sea-surface temperature across the ocean basin affects the weather of the surrounding continents.

In 2019, the IOD started weakly positive and became progressively more positive from May to October, ultimately becoming one of the strongest positive IOD events since reliable records began around 1960. The IOD index declined somewhat before the end of the year. The positive phase of the IOD during austral winter and spring has been associated with drier and warmer conditions over Indonesia and surrounding countries, as well as parts of Australia. Indeed, Australia has seen unusually dry conditions during winter and spring exacerbating long-term rainfall deficits. The positive IOD is also linked to late withdrawal of the south-west Indian monsoon, as was observed this year, and to high rainfall in the later part of the year in east Africa. For more details on regional impacts, see the following sections: Heavy rainfall and floods, Drought and Case study: Severe climatic shocks lead to a deterioration of the food security situation and to population displacement in the Greater Horn of Africa in 2019.

HIGH-IMPACT EVENTS IN 2019

The following sections describe some of the high-impact events that occurred in 2019. Information on such events is largely based on contributions from WMO Members with additional information from the Global Precipitation Climatology Centre (GPCC), Regional Climate Centres and tropical storm monitoring centres.

HEAT AND COLD WAVES

The year 2019 also saw numerous major heatwaves. Amongst the most significant were two heatwaves that occurred in Europe in late June and late July (Figure 16). The first one reached its maximum intensity in southern France, where a national record of 46.0 °C (1.9 °C above the previous record) was set on 28 June at Vérargues (Hérault). It also affected much of western Europe. The second one was more extensive, with national records set in Germany (42.6 °C), the Netherlands (40.7 °C), Belgium (41.8 °C), Luxembourg (40.8 °C) and the United Kingdom (38.7 °C). The heat also extended to the Nordic countries, where Helsinki had its highest temperature on record (33.2 °C) on 28 July. At some long-term stations, records were broken by 2 °C or more, including Paris, where a temperature of 42.6 °C, at the main Montsouris observatory on 25 July, was 2.2 °C above the previous record set in 1947, and Uccle (near Brussels), whose 39.7 °C was 3.1 °C above the previous record (for impacts, see the section Extreme heat and health).

Japan experienced two heatwaves that were notable in different ways. The first occurred in late May, with unusually high temperatures, including 39.5 °C (the equal highest on record for any time of year on the island of Hokkaido), but limited impacts. The second, in July, was less unusual in a meteorological sense but had much greater health impacts as it occurred during the peak of summer and was focused in the more heavily populated area of Honshu.

Australia had an exceptionally hot summer in 2018–2019. The mean summer temperature was the highest on record by almost 1 °C, and January was Australia's hottest month on record. Most of the country was affected,

[45] http://www.wmo.int/pages/prog/wcp/wcasp/documents/WMO_ENSO_May19_Eng.pdf

with the most extreme anomalies occurring in inland New South Wales. The heat was most notable for its persistence but there were also significant individual extremes, including 46.6 °C at Adelaide on 24 January, the city's highest temperature on record. The heat extended to New Zealand at the end of January, with record highs on 29 January at Hamilton (32.9 °C) and Wellington (30.3 °C), and significant wildfires in the north of South Island. There was further extreme heat in December, which was the hottest on record for Australia and included Australia's hottest area-averaged day on record (41.9 °C) on 18 December, whilst Nullarbor Roadhouse reached 49.9 °C on 19 December, the highest temperature in Australia since 1998. In total, Australia's seven hottest days on record, and nine of the ten hottest, occurred in 2019.

Another major heatwave of the southern hemisphere summer occurred in southern South America in late January and early February. The initial stage of the heatwave peaked in central Chile, with records set in a number of locations, including Santiago (38.3 °C on 27 January). The following week, exceptionally high temperatures reached the far south of the continent: 30.8 °C at Rio Grande (Argentina, 53.8° S), on 4 February, is believed to be the southernmost recorded instance of a temperature of 30 °C.

Whilst the absolute highest temperatures in the Middle East were not as high as some observed in recent years, some were noteworthy: 49.9 °C at Sedom, on 17 July, was Israel's highest temperature since at least 1942. Extreme heat also affected India in the pre-monsoon period in May and early June. A number of record-high temperatures were set, including 48.0 °C at New Delhi Airport on 10 June.

Consistent with a warm year globally and an overall warming trend, extreme cold was less common than extreme heat. One area of below-average temperature for 2019 was North America (Figure 2). The year's most significant cold spell was in late winter in central North America. This started with an intense cold wave in the United States Midwest in late January, including an Illinois state record of –38.9 °C at Mount Carroll on 31 January, followed by very persistent cold through February and early March in inland western areas on both sides of the United States-Canada border. February mean temperatures were more than 15 °C below normal in places, including Great Falls (Montana), whose monthly mean of –17.9 °C was 15.3 °C below normal and more than 5 °C below the previous record. It was also the coldest February on record for several regions in western Canada, including the city of Vancouver, and the first half of the year in parts of eastern Canada was rather cold.

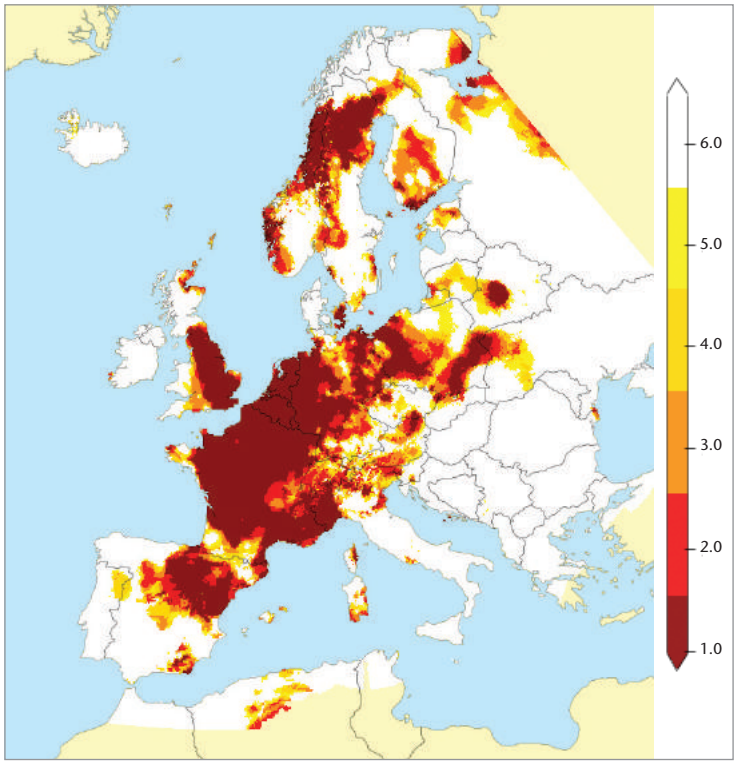

Figure 16. Ranking of the highest June and July 2019 temperatures in Europe with respect to a record that begins in 1950. The darkest shades of red indicate record-breaking values *(Source: E-OBS dataset, Royal Netherlands Meteorological Institute (KNMI), http://surfobs.climate.copernicus.eu/stateoftheclimate/july2019.php).*

There were further outbreaks of unseasonable cold and early-season snowfall in the western and central interior of North America in late September and late October. Record-low temperatures for October were set for eight states in the northern and western United States late in the month, in marked contrast to the record-high temperatures for the month set in ten southern and eastern states early in the month. Heavy snow in mid-October, with falls of up to 74 cm, caused major disruption and power outages in Manitoba (Canada). The first half of November was also unusually cold in many parts of the northern United States and southern Canada.

While temperatures were near or above average, very heavy winter and early spring precipitation led to an unusually heavy snowpack in many parts of the European Alps. More than 300 cm of snow fell in parts of the Austrian Alps between 4 and 15 January, whilst spring snowfalls led to

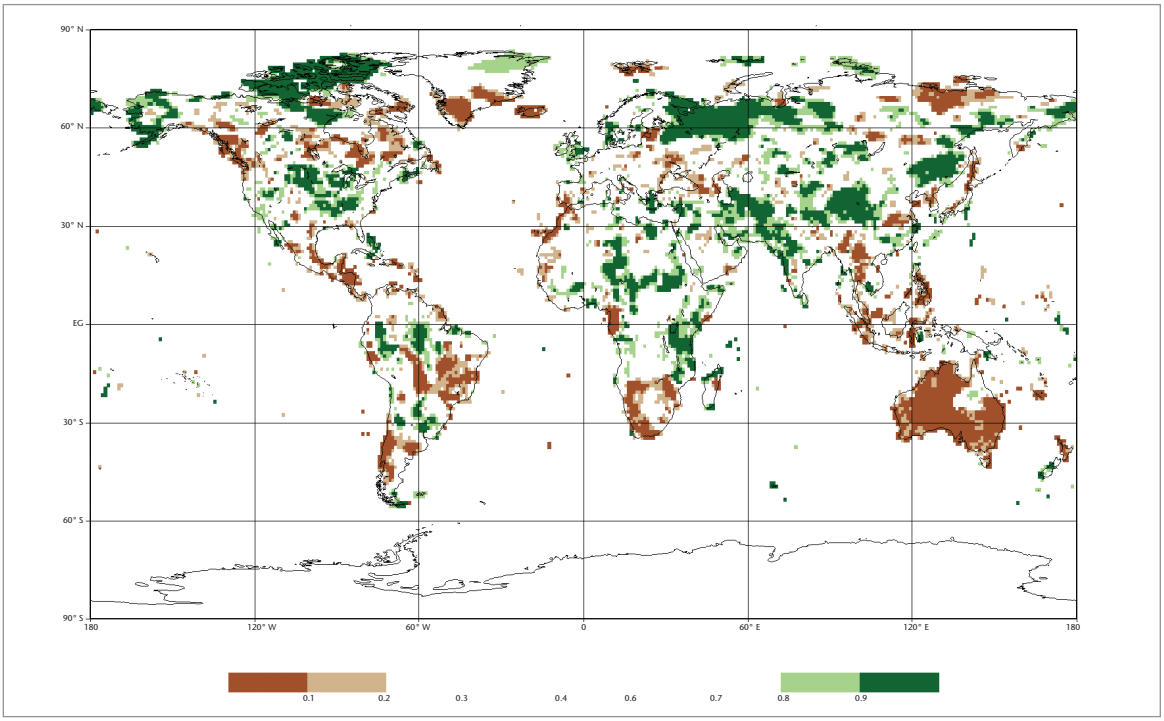

Figure 17. Annual total precipitation in 2019, expressed as a percentile of the 1951–2010 reference period, for areas that would have been in the driest 20% (brown) and wettest 20% (green) of years during the reference period, with darker shades of brown and green indicating the driest and wettest 10%, respectively *(Source: Global Precipitation Climatology Centre (GPCC), Deutscher Wetterdienst, Germany).*

a record-high snow depth for 1 June of 270 cm at Weissfluhjoch (Switzerland, 2540 m elevation), although very hot weather in June led to that snow melting by early July, close to the normal start of the snow-free period. Numerous avalanches were reported throughout the region during the heaviest snowfall periods.

PRECIPITATION

Unusually dry conditions in relation to long-term means for 2019 (Figure 17) were observed in Australia and western Indonesia and surrounding countries. Also, southern Africa, Central America and parts of South America received abnormally low precipitation amounts. Large areas with unusually high precipitation amounts were observed in the Central United States, Northern Canada, northern Russia, South-west Asia, northern China and eastern Africa.

There was a large precipitation deficit in India in June as the onset of the monsoon was delayed. However, associated with the positive IOD phase, the withdrawal of the Indian monsoon was also delayed and there was an excess of precipitation in the following months for all regions except north-east India. In addition, positive precipitation anomalies in eastern Africa and negative anomalies in the Malay Archipelago and Australia are associated with the positive IOD phase, which prevailed through most of the second half of 2019.

The longest period of consecutive wet days (CWD) in 2019 was longer than average[46] in tropical South America, tropical western Africa, tropical South-east Asia and the Maritime Continent. In 2019, the longest period of consecutive dry days (CDD) was longer than normal in Australia, southern and western Africa, central and southern South America and northern North America. The period of CDD was shorter than normal in South-west Asia and the Arabian Peninsula, south-west North America and the northern Andes region. The number of heavy precipitation days (days with more than 20 mm precipitation, PD20) was above the long-term means in India, parts of eastern Africa, parts of South America, central North America and parts of eastern Asia. Fewer than normal heavy precipitation days were observed in the Maritime Continent, central Africa and Madagascar as well as in parts of tropical South and Central America.

[46] Long-term means of the mentioned extreme indices are referenced to the period 1982–2016 and were calculated as follows: The extreme index was first calculated for each year in this 35-year period, then the mean of these 35 values was referenced as long-term mean. This non-standard definition of a long-term mean is due to the availability of reliable gridded data.

HEAVY RAINFALL AND FLOODS

Regular flooding occurred during the Indian summer monsoon season, particularly in western and northern India and neighbouring countries. Overall, all-India rainfall for the summer monsoon season (June–September) was 10% above the 1961–2010 average, the first above-average year since 2013 and the wettest since 1994, despite below-average June rainfall. The retreat of the monsoon was also exceptionally late, the withdrawal date of 9 October being the latest on record. Over 2 200 lives were reported to have been lost in various flooding episodes in India, Nepal, Bangladesh and Myanmar during the season. Monsoonal flooding also affected parts of southern China in June, with 83 deaths and over US$2.5 billion in economic losses reported.[47]

The Islamic Republic of Iran was badly affected by flooding in late March and early April, with the Shiraz region being the worst affected. During the event, 24-hour rainfall totals were as high as 188 mm. At least 76 deaths were reported as well as severe economic losses.

A tropical low brought extreme rainfall and associated flooding in northern Queensland (Australia) in late January and early February. Rainfall totals over a 10-day period exceeded 2000 mm in some coastal areas around Townsville, with Townsville itself receiving 1 259.8 mm,[48] whilst a second episode of heavy rain in inland north-west Queensland brought 7-day totals exceeding 600 mm. There was major urban flooding in the Townsville area, whilst in north-west Queensland some rivers expanded to tens of kilometres in width. The flooding and associated unusually cool weather led to heavy livestock losses. Total economic losses were estimated to be in the order of US$2 billion.[49]

In March, flash flooding and associated landslides occurred around Jayapura, in the Indonesian province of Papua, after rainfall of 235 mm in 8 hours, with at least 112 deaths reported. Later, an influx of tropical moisture brought extreme rainfall to the west coast of New Zealand's South Island in late March, with a national 48-hour record of 1086 mm at Cropp River and associated major flooding. A bridge on the region's main highway was washed away.

Persistent heavy rainfall affected a large part of the central United States in late 2018 and the first half of 2019. The 12-month rainfall averaged over the contiguous United States for the period July 2018 to June 2019 (962 mm) was the highest on record. This led to long-lived flooding in the Mississippi basin, with the river remaining above flood stage at Baton Rouge (Louisiana) for nearly seven months, from 6 January to 4 August. There was also significant flooding in parts of eastern Canada in April and early May, due to a combination of heavy rain and rapid melting of an above-average snowpack, particularly in the Ottawa and Montreal areas and in New Brunswick, with 6 000 dwellings flooded in the Ottawa region. Total economic losses from flooding in the United States, in 2019, were estimated at US$20 billion,[50] with especially acute episodes on the Missouri River in March, and the Arkansas River in late May and early June.

Very wet conditions affected parts of South America in January. There was major flooding in northern Argentina, Uruguay and southern Brazil, with losses in Argentina and Uruguay estimated at US$2.5 billion. January monthly totals exceeded 600 mm at a number of sites in north-east Argentina.

In October and November, major flooding affected many hitherto drought-affected parts of east Africa (see Case study: Severe climatic shocks lead to a deterioration of the food security situation and to population displacement in the Greater Horn of Africa in 2019). Earlier in the year, flooding during the rainy season affected a number of countries, including Sudan, Nigeria, Cameroon and Côte d'Ivoire, although overall Sahel seasonal rainfall was mostly fairly close to average.

---

[47] Emergency Events Database (EM-DAT), Centre for Research on the Epidemiology of Disasters (CRED).

[48] http://www.bom.gov.au/climate/current/statements/scs69.pdf

[49] http://thoughtleadership.aonbenfield.com/Documents/20191107_analytics-if-october-global-recap.pdf

[50] https://www.ncdc.noaa.gov/billions/events/US/2019

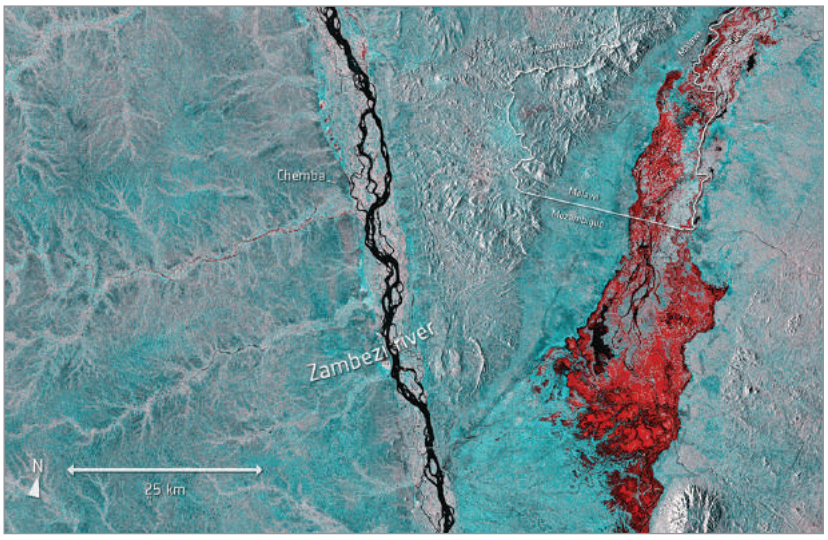

Figure 18. Flooding from Cyclone *Idai*. The image is from Copernicus Sentinel-1 and shows part of the flooding, depicted in red, to the east of the Zambezi River in Mozambique and Malawi. The picture comprises two satellite images, one from 2 March, before the cyclone hit the region, and another from 20 March, in the wake of the cyclone (Copernicus, https://www.esa.int/ESA_Multimedia/Images/2019/03/Flooding_following_Cyclone_Idai)

TROPICAL CYCLONES

Global tropical cyclone activity in 2019 was above average. The northern hemisphere had 72 tropical cyclones, compared with the average of 59, although accumulated cyclone energy (ACE) was only 4% above average. The 2018–2019 southern hemisphere season was also above average, with 27 cyclones, the highest number in a season since 2008–2009.

It was a particularly extreme cyclone season in the North Indian Ocean. Three cyclones reached maximum sustained winds of 100 kn or more, the first known instance in a single season, and the seasonal ACE was the highest on record by a large margin. *Fani* was the most significant cyclone to affect India since 2013, making landfall in the east, on the Odisha coast, on 3 May, with sustained winds of 100 kn, having earlier peaked at 135 kn in the Bay of Bengal. There was significant damage in coastal areas and loss of life, although extensive evacuations in affected coastal areas greatly reduced the human impact. *Kyarr*, in October, was one of the strongest cyclones on record in the Arabian Sea, but did not make landfall, although associated high seas and storm surges affected some coastal areas.

The South Indian Ocean basin also had an active season; there were 18 cyclones of which 13 reached hurricane intensity, equalling the largest number on record. Tropical Cyclone *Idai* made landfall near Beira (Mozambique) on 15 March (Figure 18), after maximum sustained winds of 105 kn. It was one of the strongest known cyclones to make landfall on the east coast of Africa. There was widespread destruction from wind and storm surge in coastal Mozambique, especially in the city of Beira, whilst severe flooding extended to inland regions of Mozambique and parts of Zimbabwe, particularly the north-east. Over 900 deaths were associated with the storm, the greatest known loss of life in a southern hemisphere tropical cyclone in at least the last 100 years. The following month, severe Cyclone *Kenneth* made landfall in a more sparsely populated region of northern Mozambique where damage was less severe.

One of the year's most intense Tropical Cyclones was *Dorian*, which reached category 5 intensity in the western Atlantic at the end of August, making landfall in the Bahamas on 1 September, with maximum sustained winds of 165 kn, equalling the highest on record for a North Atlantic landfall. *Dorian* was also exceptionally slow-moving and remained near-stationary over the Bahamas as a category 5 system for about 24 hours. The prolonged extreme winds and storm surge led to near-total destruction on a number of islands of the Bahamas, with at least 60 deaths reported[51] and economic losses estimated at more than US$ 3 billion.[52] *Dorian* then moved north-east, with significant damage recorded on parts of the United States east coast and in the Canadian province of Nova Scotia. Tropical Storm *Imelda* brought extreme rainfall to the eastern border of Texas, also hit by Hurricane *Harvey* in 2017, with rainfall totals of over 1000 mm in places. Estimated losses stand at US$ 5 billion.[50] The number of cyclones in the North Atlantic was well above average, but the number reaching hurricane intensity was close to normal.

Typhoon *Hagibis* made landfall west of Tokyo on 12 October, with a central pressure of 955 hPa. The major impact of *Hagibis* was flooding, as a result of extreme rainfall. Hakone, in the foothills of Mount Fuji, had a daily total of 922.5 mm, the highest on

[51] https://reliefweb.int/report/bahamas/hurricane-dorian-situation-report-14-october-15-2019

[52] https://www.iadb.org/en/damages-and-other-impacts-bahamas-hurricane-dorian-estimated-34-billion-report

record for a calendar day in Japan. Many other sites in the region west of Tokyo had daily totals in excess of 400 mm. At least 96 deaths were reported. In September, Typhoon *Faxai* contributed to major disruption in Chiba prefecture. Earlier in the season, Typhoon *Lekima* had made landfall in Zhejiang province (China) with major flooding and heavy economic losses reported. With maximum wind speed at landfall of 185 km/h, *Lekima* was the 5th strongest typhoon to make landfall in China since 1949. Overall, activity in both the North-east and North-west Pacific basins was close to average.

SEVERE STORMS

Repeated extratropical systems affected the Mediterranean region in the autumn, with extreme rainfall and high winds associated with significant damage. The most severe events affected parts of Spain, especially around the Alicante and Murcia regions, in mid-September; southern France in mid-October; and the northern Adriatic in mid-November. Events in Spain and France both brought 24-hour rainfall totals exceeding 200 mm in places, whilst a storm surge associated with the November storm raised water levels in Venice to 1.85 m, the highest since 1966 and the 2nd highest in the instrumental record. Italy saw regular flooding in November, which was the wettest on record for the Emilia-Romagna region, whilst significant flooding and wind damage was also reported in southern Austria. There were also a number of severe thunderstorms in the Mediterranean region during the summer, including near Thessaloniki (Greece) on 10–11 July, with seven deaths reported, and in Corsica (France) on 15 July, when 30 mm of rain was reported in six minutes.

Widespread severe thunderstorms and associated dust storms affected Pakistan and northern and western India in mid-April. At least 50 deaths were reported in India on 16–17 April with a further 39 in Pakistan; 60 deaths were reported from further severe thunderstorms in northern India in the first half of June.

The United States experienced its most active tornado season since 2011. May was especially active, with 556 tornadoes reported, the 2nd highest number on record for any single month. However, only one tornado reached EF-4 intensity during the year, and casualties were well below the long-term average.

DROUGHT

Drought affected many parts of south-east Asia and the south-west Pacific in 2019, associated in many cases with the strong positive IOD phase. Exceptionally dry conditions prevailed from mid-year onwards in Indonesia and neighbouring countries; Singapore had its driest July to September on record.

Further north, it was a severe drought year in many parts of the Mekong basin. The worst affected areas were near the China-Laos border, where April–September rainfall was more than 50% below normal in places, although heavy rain in central and southern Laos in September eased drought conditions there. April–July rainfall in Yunnan province of China was the lowest since 1961. It was also abnormally dry in parts of northern Thailand, with January–September rainfall at Chiang Rai 42% below normal. The Mekong River was at or near the lowest levels observed for the time of year in the last 30 years at various locations in the second half of 2019.

Long-term drought conditions, which had affected many parts of inland eastern Australia in 2017 and 2018, expanded and intensified in 2019, particularly in the second half of the year, which saw Australia's driest spring (November and December) on record. The worst affected areas were in the northern half of New South Wales and adjacent border areas of Queensland, where annual rainfall was widely the lowest on record and up to 70%–80% below average. Some areas had only about half their previous record-low rainfall. Most of the country had well below-average rainfall (Figure 19), with the only above-average areas being in northern Queensland, affected by the early 2019 floods, and in western Tasmania. The 2018/2019 wet season (October–April) was also widely the driest since 1991–1992 in tropical areas of Western Australia and the Northern Territory, and was marked by an almost total lack of precipitation in the central continent. It was the driest year on record for Australia as a whole, for the Murray-Darling Basin and for the states of South Australia (where the annual total at the Marree station was only 12 mm) and New South Wales. The drought led to severe water shortages on the rivers of the northern Murray-Darling Basin,

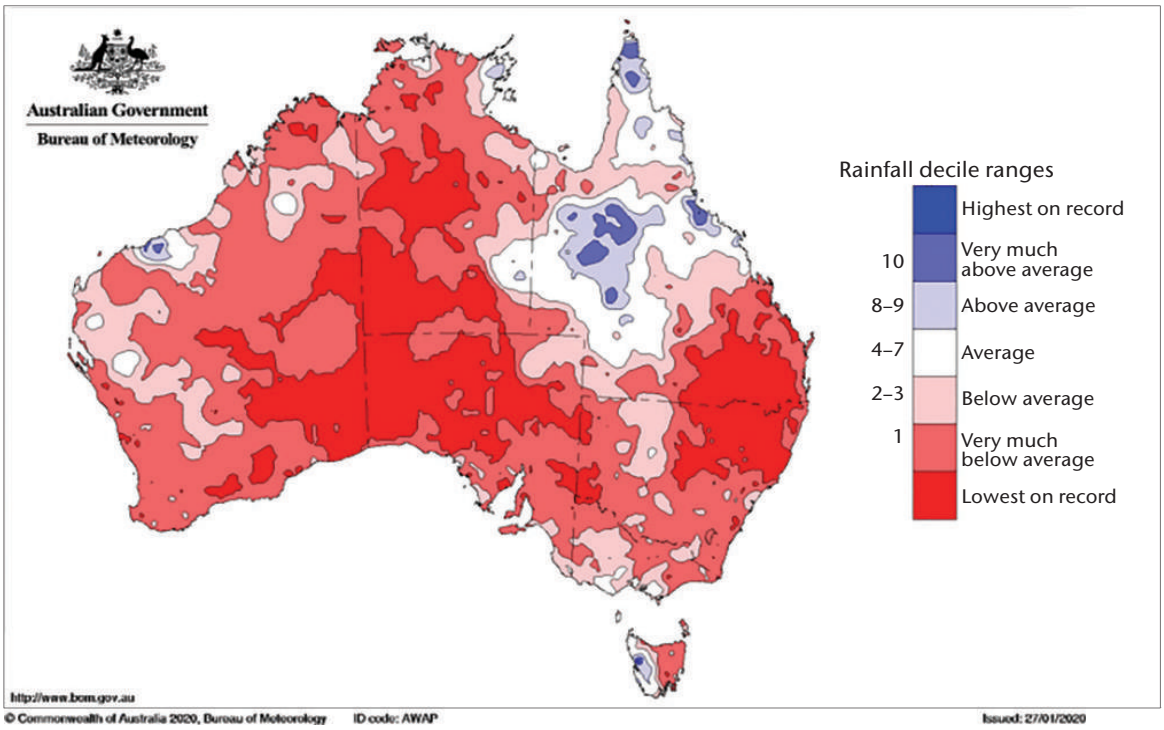

Figure 19. Rainfall deciles for Australia for the period 1 January–31 December 2019 (distribution based on gridded data) *(Source: Australian Bureau of Meteorology)*

DROUGHT MONITORING IN AUSTRALIA UTILIZING PRODUCTS FROM THE WMO SPACE-BASED WEATHER AND CLIMATE EXTREMES MONITORING DEMONSTRATION PROJECT

Yuriy Kuleshov, Lynette Bettio, Takuji Kubota, Tomoko Tashima, Pingping Xie, Toshiyuki Kurino and Peer Hechler

Recognizing the need to better utilize and improve monitoring of weather and climate extremes from space, WMO initiated the Space-based Weather and Climate Extremes Monitoring Demonstration Project (SEMDP). This project ran a demonstration phase in 2018–2019 and was focused on monitoring drought and heavy precipitation. It was implemented in WMO Regional Association II and Regional Association V and its geographical domain covers South-East Asia and the Western Pacific Ocean area, from 40° N to 45° S; 50° E to 160° W. The Japan Aerospace Exploration Agency (JAXA) and the Climate Prediction Center, National Oceanic and Atmospheric Administration (CPC/NOAA) provide tailored satellite data and products for the SEMDP region.

Monthly average precipitation in the SEMDP region for June 2019 shows very low rainfall (less than 1 mm/day) over most of Australia. Most areas received only 25% to 50% of normal rainfall in the month of June. This rainfall deficit, accumulated over a number of consecutive months, resulted in drought conditions classified as severely dry and extremely dry (Standardized Precipitation Index (SPI) values below –1.5 and –2.0, respectively).

Routine examination of space-based and in situ observations showed good agreement over the Murray-Darling Basin, in south-eastern Australia, where the density of surface-based observations is high. However, there are noticeable discrepancies between the satellite and in situ observations over the central parts of the continent where the density of surface-based observations is very low. This project has clearly demonstrated the value of space-based rainfall estimates for drought detection and monitoring, especially for regions where rain gauge observations are limited or unavailable.

with heavy agricultural losses and some towns requiring water to be trucked in after their usual water sources dried up.

The 2018/2019 rainy season was poor in many parts of southern Africa, including central and western South Africa, Lesotho, Botswana and Zimbabwe. However, there were major floods in north-east Zimbabwe in March (associated with Cyclone *Idai*), and in eastern South Africa in April, where 70 deaths were reported in KwaZulu-Natal province after daily rainfall exceeded 200 mm in places. Much of southern Africa also experienced below-average rainfall in the early part of the 2019/2020 rainy season. Rainfall during the rainy season in the western and central African Sahel was generally close to average.

Dry conditions affected many parts of Central America in 2019. Lake levels fell significantly following below-average rainfall in Panama in the first half of the year, leading to shipping restrictions in the Panama Canal.

While conditions improved in Panama from mid-year, it remained substantially drier than normal in areas further north-west, including Honduras, Guatemala, Nicaragua and El Salvador, until heavy rains in October. Central Chile also had an exceptionally dry year, with an annual total of only 82 mm in Santiago, less than 25% of the long-term average.

It was a second successive summer with extended dry periods in many parts of western and central Europe, from France to the Ukraine. Paris had 34 consecutive days without rain, from 19 August to 21 September, equalling the 2nd longest dry spell on record, following an earlier 27-day dry spell, from 21 June to 17 July (ranking 6th). Low levels in the Danube disrupted river transport in Serbia in early autumn, whilst the Wisla River in Poland reached its equal-lowest level on record in late September. It was also a dry winter in many parts of the western Mediterranean: rainfall in Spain from January to August was 23% below average, including the driest February of the 21st century, whilst winter rainfall over most of Morocco was less than half the long-term mean. In Iceland, late spring and early summer were especially dry in the south and west. No precipitation was recorded in Stykkishólmur for 37 consecutive days, from 21 May to 26 June, the longest drought on record in the station series beginning in 1856.

WILDFIRES

Wildfires, typically in response to abnormally dry and/or warm conditions, again affected many parts of the world in 2019. Activity was lower than in recent years in some known wildfire areas, such as western North America, but major fires in California, in October, still caused significant losses. On the other hand, it was an above-average fire year in several higher-latitude regions, including Siberia (Russian Federation) and Alaska (United States), with fire activity occurring in some parts of the Arctic where it was previously extremely rare. In 2019, CO_2 emissions from summer wildfires in the Arctic were the highest in the 17-year record of the Copernicus Atmosphere Monitoring Service (CAMS)/ECMWF Global Fire Assimilation System (GFASv1.2) dataset.

Australia experienced an exceptionally prolonged and severe fire season in the later part of 2019, with repeated major outbreaks. Major fires began in north-east New South Wales and southern Queensland in early September, with further outbreaks extending progressively southwards during the following months, supported by very dry conditions and several episodes of strong westerly winds and extreme heat. The monthly accumulated Forest Fire Danger Index, an indicator of severe fire weather, for December was the highest on record for any month in Queensland, New South Wales, South Australia and the Australian Capital Territory. Many individual fires burned for two months or more. The fires reached their peak at the end of December and in the first few days of January, with widespread destruction in south-eastern New South Wales, especially near the coast, and eastern Victoria, as well as near Adelaide and on Kangaroo Island in South Australia. As of early 2020, 33 deaths had been reported and over 2 000 properties had been lost, while a total of about 7 million hectares had been burnt in New South Wales and Victoria. Earlier in 2019, a dry summer in Tasmania contributed to numerous long-lived fires in January and February, in the normally wetter western and central parts of the island. This is the second time in four years that fires have affected regions where historically fire was extremely rare.

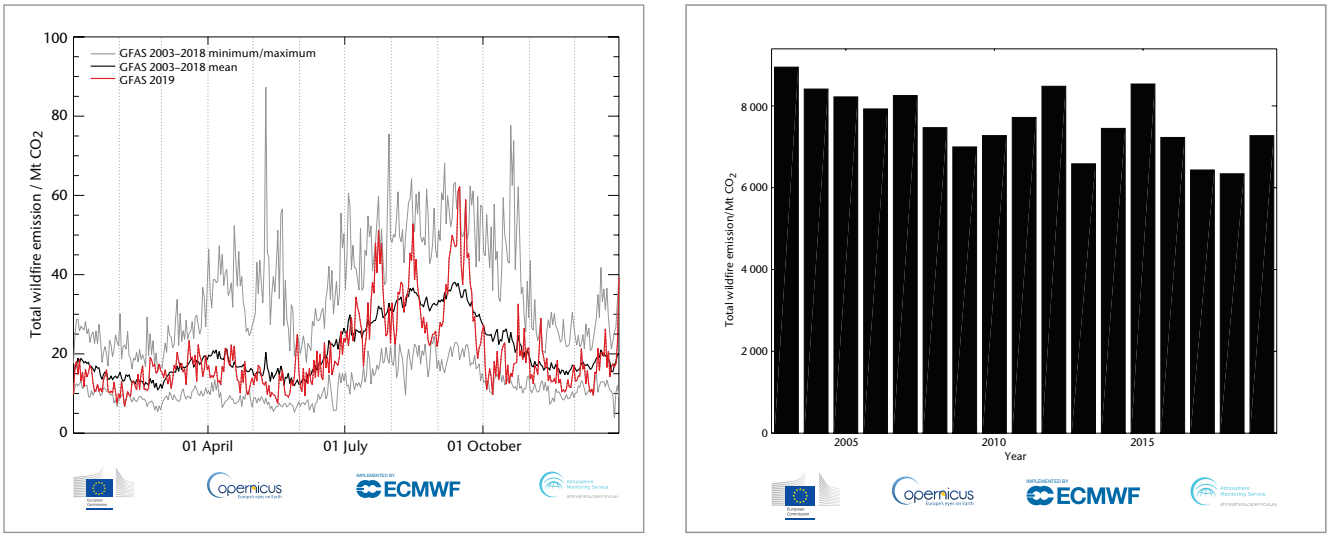

Figure 20. Left: Global daily total estimated CO_2 emissions from wildfires, in megatonnes of CO_2, from 1 January to 31 December 2019, compared to the mean and minimum/maximum daily values based on the years 2003–2018. Right: Global annual total estimated CO_2 emissions from wildfires, in megatonnes of CO_2, between 2003 and 2019. The figures are based on the CAMS/ECMWF Global Fire Assimilation System (GFASv1.2).

The severe drought in Indonesia and neighbouring countries led to the most significant fire season since 2015, although the fires and associated smoke pollution were not as severe as in 2015.[53] Fire activity in the Amazon basin was also higher than in recent years, particularly in August, although it fell well short of previous severe drought years such as 2010. The number of reported fires in Brazil's Amazonia region was only slightly above the 10-year average, but total fire activity in South America was the highest since 2010, with Bolivia and Venezuela among the countries with particularly active fire years.[54]

While 2019 witnessed significant regional wildfire activity around the world, the overall global daily and annual total estimated emissions were close to the average calculated for the previous 17 years of the CAMS/ECMWF Global Fire Assimilation System (GFASv1.2) dataset. GFASv1.2 combines active fire observations from the MODIS instruments on the NASA Terra and Aqua satellites to provide a dataset of daily average fire radiative power and estimated emissions of pyrogenic species, including particulate matter, reactive gases and greenhouse gases, as of 1 January 2003 until the time of writing.

Daily total wildfire CO_2 emissions throughout the year (Figure 20, left) generally followed the 2003–2018 mean with increased activity, greater than 20 Mt CO_2 per day, between June and October, and reduced activity, less than 20 Mt CO_2 per day, throughout the rest of the year. The largest increases above the 17-year mean occurred in July, August, September and at the end of December, corresponding to the peak activity of wildfires in the Arctic, Siberia, Indonesia and Australia respectively.

The global annual total CO_2 emissions from wildfires for 2019 (Figure 20, right) were higher than the previous two years but remained lower than most other years in the dataset, consistent with the general decline in global wildfire activity since 2003.

[53] http://asmc.asean.org/asmc-haze-hotspot-annual-new#Hotspot

[54] From the National Institute for Space Research (INPE), Brazil.

Climate-related risks and impacts

The risk of climate-related impacts depends on complex interactions between climate-related hazards and the vulnerability, exposure and adaptive capacity of human and natural systems.[55] At current levels of global greenhouse gas emissions, the world remains on course to exceed the agreed temperature thresholds of either 1.5 °C or 2 °C above pre-industrial levels,[56] which would increase the risk of pervasive effects of climate change beyond what is already seen.[57,58]

Climate-related events already pose risks to society through impacts on health, food and water security as well as human security, livelihoods, economies, infrastructure and biodiversity. Climate change also has severe implications for ecosystem services. It can affect patterns of natural resource use, as well as the distribution of resources across regions and within countries.

HEALTH AT INCREASING RISK

Health effects include heat-related illness and death; injury and loss of life associated with severe storms and flooding; occurrences of vector-borne and water-borne diseases; exacerbation of cardiovascular and respiratory diseases through air pollution; and stress and mental trauma from displacement as well as loss of livelihoods and property.

EXTREME HEAT AND HEALTH

Highly-populated areas of the planet are increasingly exposed to warmer conditions, experiencing a mean summer temperature change that is higher than the global average (Figure 21).

Extreme heat conditions are taking an increasing toll on human health and health systems. Even greater consequences are

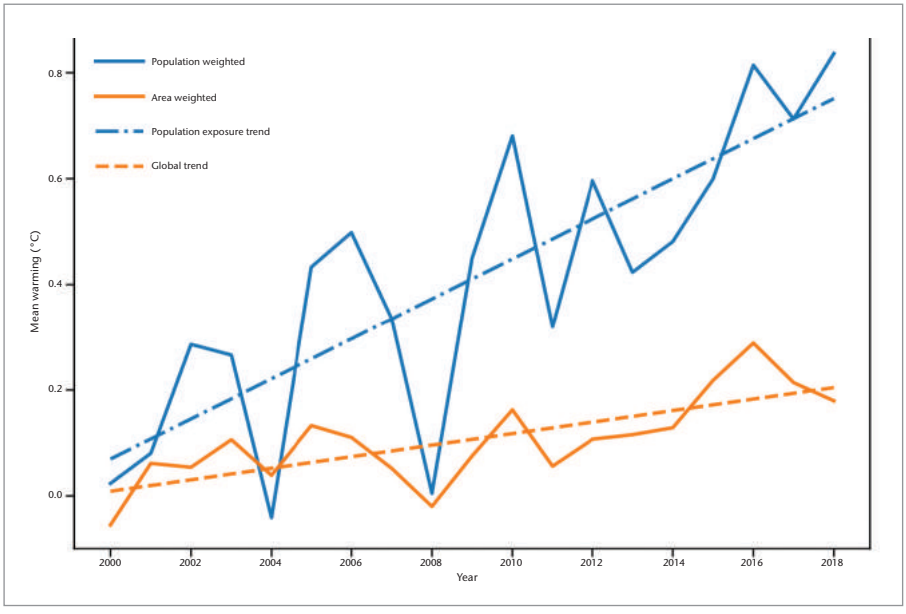

Figure 21. Population vs area weighted mean summer warming (June–August in the northern hemisphere, December–February in the southern hemisphere), relative to the 1986–2005 average.[59]

[55] United Nations Environment Programme (UNEP), 2019: *Global Environment Outlook – GEO-6: Healthy Planet, Healthy People* (Ekins P., J. Gupta and P. Boileau, eds.), 745 pages. Cambridge, Cambridge University Press, doi 10.1017/9781108627146, https://www.unenvironment.org/global-environment-outlook

[56] Intergovernmental Panel on Climate Change (IPCC), 2018: *Global Warming of 1.5 °C* (Masson-Delmotte, V., P. Zhai, H.-O. Pörtner, D. Roberts, J. Skea, P.R. Shukla, A. Pirani, W. Moufouma-Okia, C. Péan, R. Pidcock, S. Connors, J.B.R. Matthews, Y. Chen, X. Zhou, M.I. Gomis, E. Lonnoy, T. Maycock, M. Tignor, and T. Waterfield, eds.). Geneva, https://www.ipcc.ch/sr15/

[57] United Nations Environment Programme (UNEP), 2019: *Emissions Gap Report 2019*. Nairobi, https://www.unenvironment.org/resources/emissions-gap-report-2019

[58] United Nations Environment Programme (UNEP), 2019: *Lessons from a Decade of Emission Gap Assessments* (J. Christensen and A. Olhoff, eds). Nairobi.

[58] Watts, N. et al., 2019: The 2019 report of *The Lancet* Countdown on health and climate change: ensuring that the health of a child born today is not defined by a changing climate. *The Lancet*, 394 (10211), pp. 1836-1878, https://www.thelancet.com/journals/lancet/article/PIIS0140-6736(19)32596-6/fulltext.

recorded in locations where extreme heat occurs in the context of aging populations, urbanization, urban heat island effects and health inequalities.[60] In 2018, vulnerable people over the age of 65 experienced a record 220 million more heatwave exposure,[61] than the average for the baseline of 1986–2005 — breaking the previous record set in 2015 by 11 million.

In 2019, record-setting high temperatures in Australia, India, Japan and Europe adversely affected health and well-being. A major heatwave affected Japan in late July and early August 2019, resulting in over 100 deaths and placing a great burden on the health system with an additional 18 000 hospital admissions. Europe experienced two significant heatwaves in the summer of 2019. In June, a heatwave affecting south-western and central Europe resulted in a number of deaths in Spain and France. The more significant heatwave occurred in late July, affecting much of central and western Europe. In the Netherlands, this event was associated with 2 964 deaths, nearly 400 more deaths than during an average summer week,[62] while in England 572 (390 to 754, 95% confidence interval) excess deaths were observed above the baseline for all-cause mortality in people over 65.[63]

In metropolitan France, between the beginning of June and mid-September, over 20 000 emergency room visits and 5 700 home visits by doctors were recorded for heat-related illnesses.[64] During the two summer heatwaves, a total of 1 462 excess deaths (a 9.2 % increase in average mortality, with an uncertainty range of 548 to 2 221 excess deaths) were observed in the affected regions. Older people over 75, but also age groups 15–44 and 65–74 were those mostly affected. In regions of France that experienced extreme heat (red alerts), 572 observed excess deaths represent a 50% increase in the mortality that would have been expected if no heatwave had occurred.

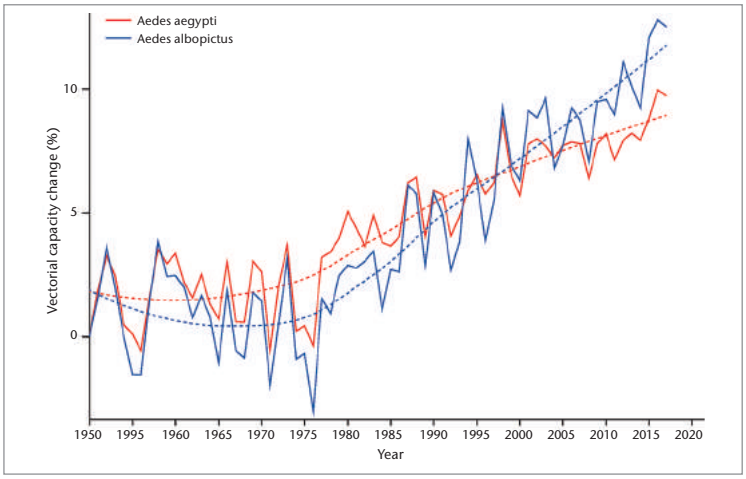

Figure 22. Changes in global vectorial capacity for the dengue virus vectors *Aedes aegypti* and *Aedes albopictus* since 1950. Vectorial capacity depends on temperature and is calculated using historical climate data.[59]

VECTOR-BORNE DISEASES

Changes in climatic conditions since 1950 are making it easier for the Aedes mosquito species to transmit the dengue virus, increasing the risk of the disease (Figure 22). In parallel, the global incidence of dengue has grown dramatically in recent decades, and about half of the world's population is now at risk of infection.[65] In 2019, the world experienced a large increase in dengue cases, compared with the same period in 2018. The Americas identified more than 2 800 000 suspected and confirmed dengue cases, including around 1 250 deaths.[66] In the three months from August to October, 85% of nearly 1 050 000 cases were reported by Brazil, the Philippines, Mexico, Nicaragua, Thailand, Malaysia and Colombia.[67]

---

[60] Sera, F. et al., 2019: How urban characteristics affect vulnerability to heat and cold: a multi-country analysis. *International Journal of Epidemiology*, 48(4):1101-1112, doi: 10.1093/ije/dyz008, https://www.ncbi.nlm.nih.gov/pubmed/30815699.

[61] Each heatwave exposure is one person over 65 experiencing one heatwave (defined as a period of 3 or more days at a given location where the minimum daily temperature was greater than the 99th percentile of the distribution of minimum daily temperature for the summer months 1986–2005).

[62] https://www.cbs.nl/en-gb/news/2019/32/more-deaths-during-recent-heat-wave

[63] https://www.gov.uk/government/publications/phe-heatwave-mortality-monitoring

[64] https://www.santepubliquefrance.fr/determinants-de-sante/climat/fortes-chaleurs-canicule/documents/bulletin-national/bulletin-de-sante-publique-canicule.-bilan-ete-2019

[65] https://www.who.int/news-room/fact-sheets/detail/dengue-and-severe-dengue

[66] https://www.paho.org/hq/index.php?option=com_content&view=article&id=6306:2011-archive-diseases-dengue&Itemid=41184&lang=en

[67] https://www.ecdc.europa.eu/en/dengue-monthly (November 22, 2019 Update)

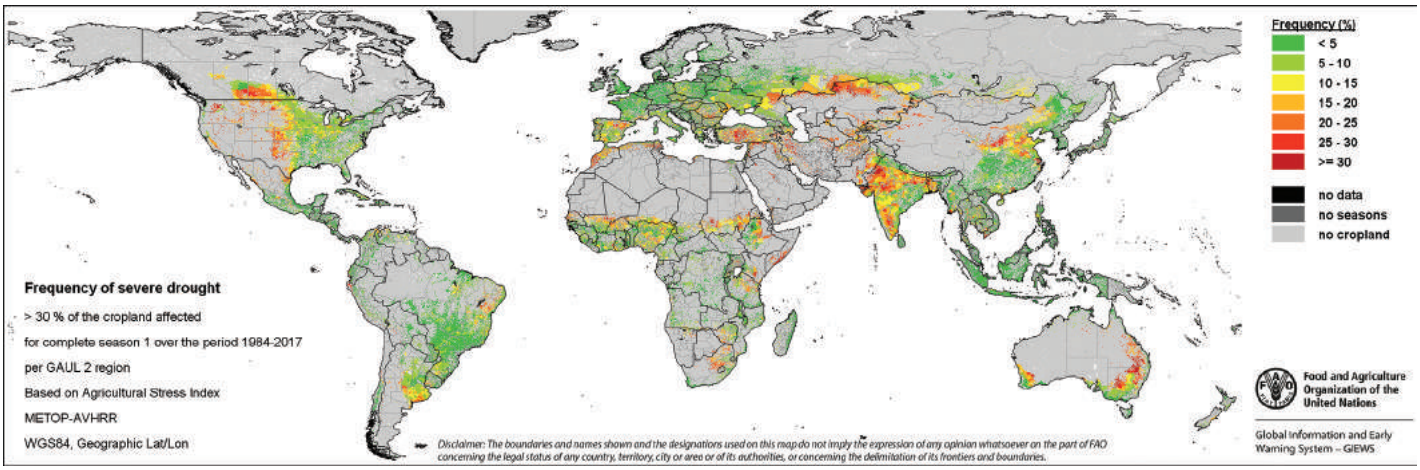

Figure 23. Frequency of severe drought in cereal-growing areas of the globe calculated using remote-sensing data in the period 1984–2017 *(Source: Food and Agriculture Organization of the United Nations (FAO), Global Information and Early Warning System (GIEWS) Earth Observations)*

FOOD SECURITY AND POPULATION DISPLACEMENT CONTINUE TO BE ADVERSELY AFFECTED BY CLIMATE VARIABILITY AND EXTREME WEATHER

Rising global temperature and changing rainfall patterns have already affected terrestrial ecosystems such as forests and grasslands, as well as agricultural lands and crop yields.[68] Between 2006 and 2016, agriculture (crops, livestock, forestry, fisheries and aquaculture) in developing countries accounted for an estimated 26% of total loss and damage incurred during medium- and large-scale climate-related disasters. While about two-thirds of loss of and damage to crops was associated with floods, almost 90% of loss and damage in the livestock sector was attributable to drought[69] (Figure 23).

In addition to conflicts, insecurity, and economic slowdowns and downturns, climate variability and extreme weather events are among the key drivers of the recent rise in global hunger and one of the leading causes of severe crises. After a decade of steady decline, hunger is on the rise again – over 820 million, or one in every nine people in the world, suffered from hunger in 2018, the latest global data available (Figure 24). The situation is most acute in sub-Saharan Africa, where the number of undernourished people increased by more than 23 million between 2015 and 2018, particularly in countries affected by conflict. Among 33 countries with food crises in 2018, climate variability and weather extremes were a compounding factor together with economic shocks and conflict in 26 countries, and the leading driver in 12 of the 26.[70] In light of this, the global community faces an enormous challenge to meet the Zero Hunger target of the 2030 Agenda for Sustainable Development.

More than 6.7 million new internal disaster displacements were recorded between January and June 2019, triggered by hydrometeorological events such as Cyclone *Idai* in south-east Africa, Cyclone *Fani* in South Asia, Hurricane *Dorian* in the Caribbean, and flooding in Iran, the Philippines and Ethiopia, generating acute humanitarian and protection needs.[71] This number was forecast

[68] Intergovernmental Panel on Climate Change (IPCC), 2019: *Climate Change and Land: an IPCC special report on climate change, desertification, land degradation, sustainable land management, food security, and greenhouse gas fluxes in terrestrial ecosystems* (P.R. Shukla, J. Skea, E. Calvo Buendia, V. Masson-Delmotte, H.-O. Pörtner, D. C. Roberts, P. Zhai, R. Slade, S. Connors, R. van Diemen, M. Ferrat, E. Haughey, S. Luz, S. Neogi, M. Pathak, J. Petzold, J. Portugal Pereira, P. Vyas, E. Huntley, K. Kissick, M. Belkacemi, J. Malley, eds.). Geneva, https://www.ipcc.ch/srccl/.

[69] Food and Agriculture Organization of the United Nations (FAO), 2018: *The impact of disasters and crises on agriculture and food security 2017*, http://www.fao.org/3/I8656EN/i8656en.pdf.

[70] Food and Agriculture Organization of the United Nations (FAO), International Fund for Agricultural Development (IFAD), United Nations Children's Fund (UNICEF), World Food Programme (WFP) and World Health Organization (WHO), 2019: *The State of Food Security and Nutrition in the World 2019: Safeguarding against economic slowdowns and downturns*. Rome, FAO.

[71] http://www.internal-displacement.org/publications/internal-displacement-mid-year-figures-january-june-2019

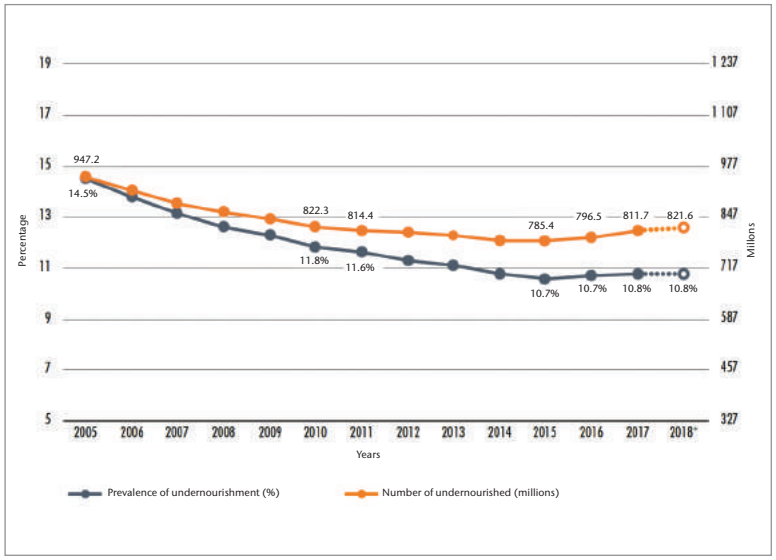

Figure 24. The number of undernourished people in the world has been on the rise since 2015. Values for 2018 are projections as illustrated by dotted lines and empty circles *(Source: Food and Agriculture Organization of the United Nations (FAO)).*

to reach close to 22 million in 2019,[72] while it reached 17.2 million across 148 countries and territories in 2018. Of all natural hazards, floods and storms have contributed the most to displacement recorded in 2019, followed by droughts. The Office of the United Nations High Commissioner for Refugees (UNHCR) was actively involved in protecting and supporting people displaced in this context, notably in Mozambique after Cyclone *Idai*.

The effects of climate-related events and disasters on the displacement of people are not the same everywhere. Asia and the Pacific remain the regions most prone to sudden and slow-onset disasters. For instance, more than 2 million people were evacuated in Bangladesh, the second most disaster-prone country in the region, due to Cyclone *Bulbul* in November 2019, and more than 2 million in China, due to Typhoon *Lekima* in August 2019. Latin America and the Caribbean were also particularly affected by climate-related events and other hazards such as volcanic eruptions and earthquakes, which resulted in further displacement. For instance, around 70 000 people became homeless in the Bahamas, in September 2019, following Hurricane *Dorian*, and more than 42 000 were displaced in the Amazonas, in Brazil, in June 2019, due to flooding. Millions of people in the Horn of Africa and west Africa were also affected by floods.

Existing refugee populations often reside in climate "hotspots", where they are exposed to and affected by slow- and sudden-onset hazards, which can also result in secondary displacement. For instance, hundreds of thousands of Rohingya refugees who have fled into Bangladesh and are now residing in Kutupalong are routinely affected by storms and heavy rainfall and landslides. Between January and November 2019, the camps in the area were hit by floods, landslides and strong winds. The Office of the United Nations High Commissioner for Refugees and partners, therefore, made preparedness for the monsoon season a priority, including building retaining structures on hillsides, drainage, roads and bridges. Poor building quality and settlement in exposed areas have resulted in over 84 000 people being affected out of a total population of nearly 945 000.[73]

Although most disaster- and climate-related displacement is internal, displacement across borders, which may be interrelated with conflict or violence, also occurs.[74] The worsening drought and violence in Somalia drove thousands of people to flee to Ethiopia, a country that also faces adverse impacts of climate-related events. The Lake Chad region has seen desertification and deforestation associated with the shrinking of Lake Chad, extreme climate events, population growth and unregulated irrigation. All of this, added to violence, which has driven millions of people from their homes in Chad, Cameroon, Nigeria and Niger, exacerbates forced displacement, including refugee movements, across borders.[75]

In southern Africa, the start of the seasonal rains was delayed, and there were extensive dry periods. In May 2019, Namibia declared

[72] Internal Displacement Monitoring Centre (IDMC), http://www.internal-displacement.org/.

[73] http://iom.maps.arcgis.com/apps/MapSeries/index.html?appid=1eec7ad29df742938b6470d77c26575a

[74] Office of the United Nations High Commissioner for Refugees (UNHCR), https://www.unhcr.org/news/stories/2019/10/5da5e18c4/climate-change-and-displacement.html

[75] Internal Displacement Monitoring Centre (IDMC), http://www.internal-displacement.org/expert-opinion/looking-beyond-boko-haram-in-the-lake-chad-region; UNHCR, https://www.unhcr.org/news/stories/2019/10/5da5e18c4/climate-change-and-displacement.html

a state of emergency in response to the drought it was facing.[76] Regional cereal output is forecast to be about 8% below the five-year average, with 12.5 million people in the region expected to experience severe food insecurity up to March 2020, an increase of more than 10% on the previous year.

Food security has been deteriorating in several areas of Ethiopia, Somalia, Kenya and Uganda due to a poor, long *Gu* rainy season, which followed a below-average 2018 short *Deyr* season. In addition, between October 2019 and January 2020, the region faced widespread flooding that affected 3.4 million people.[77]

In March 2019, Tropical Cyclone *Idai* contributed to complete destruction of close to 780 000 ha of crops in Malawi, Mozambique and Zimbabwe, further undermining a precarious food security situation in the region.[78] The cyclone also led to the displacement of at least 50 905 people in Zimbabwe,[79] 53 237 in southern Malawi[80] and 77 019 in Mozambique.[81] Furthermore, Mozambique was hit by Cyclone *Kenneth* a few weeks later, contributing to a current total of 88 381 internally displaced persons, mostly concentrated in the Beira and Quelimane areas.[82]

Food insecurity remained severe in South Sudan throughout 2019, with 4.54 million people estimated to be severely food insecure between September and December. However, the actual number of food-insecure people is likely to be substantially higher than the estimate produced in August, as widespread floods in September and October affected about 900 000 people and resulted in significant crop and livestock losses.[83]

Flash floods in Afghanistan, in March 2019, following an intense drought from April to October 2018, resulted in the worst flooding in a decade in some parts of the country: 13.5 million people are food insecure, with 22 out of 34 provinces still rallying from the severe drought faced in 2018, which had already led to 32 515 people being displaced in Herat alone.[84] The situation is particularly severe because an estimated 80% of soils in the country are degraded due to cumulative years of dry conditions.[85]

Dry weather persisted throughout the first half of 2019 in the Democratic People's Republic of Korea after two consecutive years of dry conditions and irregular weather patterns. On average, only 56.3 mm of rain fell in the country from January to March 2019, which is the lowest on record since 1917. About 10 million people urgently require food assistance.[86]

In 2019, drier than normal conditions in the Dry Corridor of Central America and the Caribbean led to forest fires across northern Guatemala and Honduras, with adverse effects on crop development, and contributed to the drying up of some rivers in Honduras. After below-normal rainfall from May to August 2019, about 50 000 families lost close to 80% of their maize production in Guatemala. Significant crop losses (up to 70%

---

[76] *AfricaNews*, 6 May 2019: Namibia declares national state of emergency over drought, https://www.africanews.com/2019/05/06/namibia-declares-national-state-of-emergency-over-drought//.

[77] https://reliefweb.int/report/south-sudan/eastern-africa-region-regional-floods-and-locust-outbreak-snapshot-january-2020

[78] Food and Agriculture Organization of the United Nations (FAO), 2019: *Early Warning Early Action Report on Food Security an Agriculture* (July-September 2019). Rome, http://www.fao.org/documents/card/en/c/ca5445en/ .

[79] International Organization for Migration (IOM), https://displacement.iom.int/reports/zimbabwe-%E2%80%94-tropical-cyclone-idai-baseline-assessment-round-1-3-27-april-2019.

[80] IOM, https://displacement.iom.int/reports/malawi-%E2%80%94-tropical-cyclone-idai-multi-sectoral-location-assessments-11-april-2019.

[81] IOM, https://displacement.iom.int/reports/mozambique-%E2%80%94-cyclone-idai-response-situation-report-%E2%80%94-round-10-october-2019.

[82] IOM, https://displacement.iom.int/mozambique.

[83] Food and Agriculture Organization of the United Nations (FAO), http://www.fao.org/3/ca7236en/ca7236en.pdf

[84] IOM, https://displacement.iom.int/reports/afghanistan-%E2%80%94-drought-response-situation-report-26-april-2019

[85] FAO, 2019: *Early Warning Early Action Report on Food Security an Agriculture* (April-June 2019). Rome, http://www.fao.org/emergencies/resources/documents/resources-detail/en/c/1190473/.

[86] FAO, 2019:. *Early Warning Early Action Report on Food Security an Agriculture* (October-December 2019). Rome, http://www.fao.org/emergencies/resources/documents/resources-detail/en/c/1239932/.

and 50% for maize and beans, respectively) were also reported in Honduras under similar dry conditions. In September 2019, the government declared an emergency due to a loss of staple crops, with more than 100 000 people at risk of food insecurity. In El Salvador, over 70 000 households are estimated to be affected by a lack of food and safe drinking water.[87]

MARINE LIFE AND BIODIVERSITY THREATENED BY THE CHANGING CLIMATE AND EXTREME EVENTS

The primary pressures on living marine resources are overexploitation, pollution from land-based activities and climate change.[88] Coral reefs are the marine ecosystem most threatened by climate-related ocean change, especially ocean warming and acidification.[89,90] Coral reefs are projected to decline to 10%–30% of former cover at 1.5 °C warming, and to less than 1% at 2 °C warming.[91] Ocean acidification may also have adverse effects on other marine systems, including mussel beds and some macroalgal habitats. Fisheries are being affected by climate change in many ways.[92] As temperature and salinity profiles change with global warming, the distribution and productivity of important target species are already being reflected in changes in the distribution of fishery catches.

Long-term monitoring of the Great Barrier Reef (GBR) showed that the hard coral cover increased slightly from 11% in 2017 to 14% in 2019 in the northern GBR (Figure 25). However, these values remain close to the lowest levels recorded by the Australian Institute of Marine Science Long-Term Monitoring Program (AIMS-LTMP) since 1985, associated with the cumulative impact of cyclones and two episodes of severe coral bleaching over the period 2014 to 2019.[93] To date, recovery has been limited. Severe Tropical Cyclone *Debbie* in 2017, and the continued southward spread of crown-of-thorns starfish outbreaks, contributed to a continuing decrease of coral cover in the Central GBR. Average hard coral cover declined slightly, from 14% in 2018 to 12% in 2019. Overall, mean coral cover on reefs in the Southern GBR region continued to decline, albeit only slightly, from 25% in 2018 to 24% in 2019.

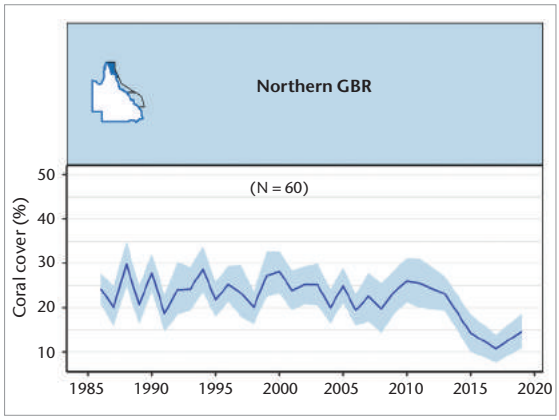

Figure 25. Trends in average hard coral cover for the northern Great Barrier Reef (GBR) based on manta-tow surveys up to June 2019. N indicates the number of reefs contributing to the analyses; blue shading represents 95% credible intervals. Note that many reefs in this region do not have a regular survey history and that in 2019 not all inshore reefs could be surveyed *(Source: Australian Institute of Marine Science (AIMS))*.[94]

[87] Ibid.

[88] Salem, H.S., 2011: Social, environmental and security impacts of climate change on the eastern Mediterranean. In: *Coping with Global Environmental Change, Disasters and Security: Threats, Challenges, Vulnerabilities and Risks* (Brauch, H.S., Spring, U.O., Mesjasz, C., Grin, J., Kameri-Mbote, P., Chourou, B., Dunay, P., Birkmann, J.,eds.). Springer, 421-445.

[89] Gattuso, J.P. et al., 2015: Contrasting futures for ocean and society from different anthropogenic CO_2 emissions scenarios. *Science*, 349(6243), doi:10.1126/science.aac4722.

[90] Albright, R. et al., 2018: Carbon dioxide addition to coral reef waters suppresses net community calcification. *Nature*, 555, 516–519, doi:10.1038/nature25968.

[91] Intergovernmental Science-Policy Platform on Biodiversity and Ecosystem Services (IPBES), 2019: *Global Assessment Report on Biodiversity and Ecosystem Services – Summary for Policymakers.* Bonn, https://ipbes.net/global-assessment.

[92] Ripple, W.et al., 2019: World Scientists' Warning of a Climate Emergency. *BioScience*, 70(1), https://doi.org/10.1093/biosci/biz088.

[93] Australian Institute of Marine Science (AIMS), 2019: *Long-term Reef Monitoring Program - Annual Summary Report on coral reef condition for 2018/19* , available at https://www.aims.gov.au/reef-monitoring/gbr-condition-summary-2018-2019.

[94] Ibid.

CASE STUDY:

Severe climatic shocks lead to a deterioration of the food security situation and to population displacement in the Greater Horn of Africa in 2019

Alessandro Costantino, Sarah Graf and Oscar Rojas, FAO

The food security situation deteriorated markedly in 2019 in some countries of the Greater Horn of Africa due to climate extremes, displacement, conflict and violence. For instance, in Somalia and Kenya, the number of people affected by food insecurity increased between late 2018 and late 2019, from 1.6 to 2.1 million and from 0.7 to 3.1 million, respectively. By late 2019, about 22.2 million people (6.7 million in Ethiopia, 3.1 million in Kenya, 2.1 million in Somalia, 4.5 million in South Sudan[95] and 5.8 million in the Sudan) were estimated to be severely food insecure,[96] only a slightly lower number than during the severe and prolonged drought of 2016–2017.[97]

Exceptional dryness prevailed in March and the first twenty days of April, with cumulative precipitation estimated to be about 80% below average across most of the Horn of Africa.[98] The unfavourable weather conditions, among the driest on record in some parts, affected several cropping areas, with reduced planted zones and yields (see Figure 26). In such dry conditions, fall armyworm infestations further constrained yields.

Above-average precipitation in late April and May reduced moisture deficits and improved vegetation conditions. Heavy showers also reduced fall armyworm infestation levels, but damage to crops was largely irreversible in several areas. The sharpest output contractions were recorded in Somalia and in south-eastern Kenya, where rainfall deficits were more severe, and the rainy season is normally shorter than in other countries in the region. In Somalia, the output of the 2019 Gu harvest was the lowest since 1995 and about 60% below the average of the previous five years. Maize production was estimated at about 50%–60% below the average in agro-pastoral and marginal agricultural areas of central, south-eastern and coastal Kenya. In pastoral areas, the exceptionally dry conditions in March and April, especially in central and northern Somalia, south-eastern Ethiopia and most of Kenya, resulted in severe weight loss and increased mortality rates in livestock as well as a sharp decline in milk production.[99] In late 2019, cereal prices were very high in most markets of Kenya, Uganda, Somalia and Ethiopia, up to twice what they had been a year earlier, thus restricting food access for large segments of the population.[100]

The 2019 October–December short *Deyr* rains were characterized by exceptionally heavy precipitation throughout the region, which received the highest or the 2nd highest rainfall

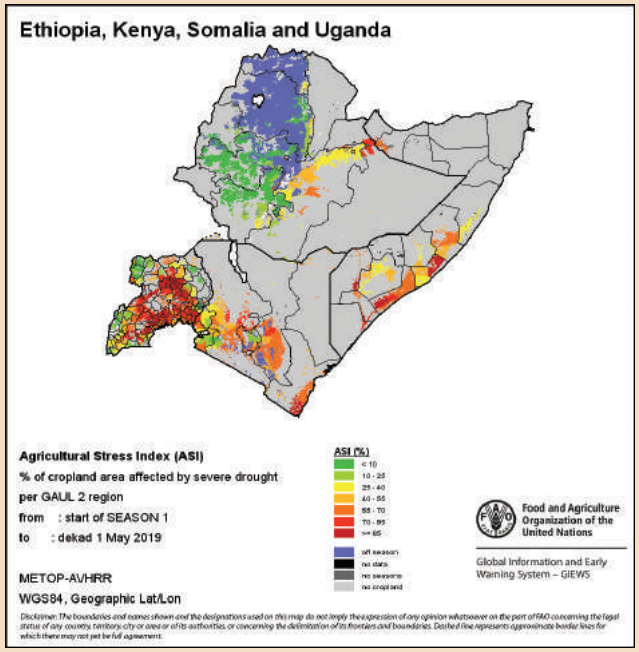

Figure 26. Agriculture Stress Index (ASI) for the Greater Horn of Africa in May 2019

[95] In South Sudan, the food insecurity projection for the October–December period, being conducted in August, does not take into account the impact of flooding, so the number of people affected by food insecurity in late 2019 is likely to be significantly higher than the estimate reported.

[96] Food and Agriculture Organization of the United Nations (FAO), 2020: GIEWS Special Alert 347: The worst desert locust outbreak in decades threatens food security across East Africa. Rome, http://www.fao.org/3/ca7610en/ca7610en.pdf.

[97] FAO, 2019: *Early Warning Early Action Report on Food Security and Agriculture* (October-December 2019). Rome, http://www.fao.org/emergencies/resources/documents/resources-detail/en/c/1239932/.

[98] FAO, *Crop Prospects and Food Situation*, July 2019, http://www.fao.org/3/ca5327en/ca5327en.pdf.

[99] FAO, *Crop Prospects and Food Situation, September 2019*, http://www.fao.org/3/ca6057en/ca6057en.pdf.

[100] FAO, *Food Price Monitoring and Analysis Bulletin*, November 2019, http://www.fao.org/3/ca6996en/ca6996en.pdf.

totals on record since 1981, between 200% and 400% of the long-term average. Atypical warming of the sea surface off the coast of East Africa, part of one of the strongest Indian Ocean Dipole (IOD) events on record, was associated with heavy rainfall inland. While abundant rains had a positive impact on crops and rangelands, they also triggered widespread floods and associated loss of life, displacement, damage to crops and livestock deaths, mainly in central and southern Somalia, south-eastern Ethiopia, northern and eastern Kenya and in South Sudan.

Climate extremes caused severe additional threats to already precarious livelihoods in East Africa and the Horn of Africa,[101] home to highly vulnerable communities with at least 75 million people living on incomes below US$ 1.9 per day.[102] An estimated 8.1 million people in the region are internally displaced, of whom at least 1.8 million are displaced by drought and 3.5 million are asylum seekers and refugees.[103] Climate and weather extremes further force people to move in search of safety: in Somalia, between January and May 2019, droughts displaced at least 60 000 people,[104] while widespread floods in October and November resulted in 370 000 additional displacements.[105] Thousands have been fleeing to Ethiopia, a country that also faces the adverse impacts of climate events, including displacement. Moreover, climate-related events are exacerbating tensions between displaced people and their host communities, further fuelling intra-communal conflict.

The country worst hit by the floods was South Sudan, where about 900 000 individuals were affected, of whom about 420 000 were displaced. Large flood-induced crop losses, especially in former Northern Bahr el Ghazal, Jonglei, Upper Nile and Warrap states, have somewhat offset the increased production and security improvements due to high yields in areas unaffected by floods. As a result, aggregate cereal production in 2019 is estimated to be higher than the poor 2018 output but below the five-year average production.[106] Significant livestock losses were reported in flood-affected areas. The flood-induced livelihood damages have further exacerbated an already dire food security situation: 4.54 million people (almost 40% of the total population) were projected to be food insecure between September and December, but the current number is likely to be substantially higher because of the floods.[107]

Uncontrolled locust reproduction in the Arabian Peninsula, coupled with unusual weather and climate conditions in East Africa, resulted in the worst desert locust outbreak in 25 years in the Horn of Africa and the most serious in 70 years for Kenya. In late 2019, the locust outbreak affected eastern Ethiopia and central/southern Somalia; by January 2020, it had spread to northern Kenya, and by June 2020 is expected to spread to southern Ethiopia, north-eastern Uganda and eastern South Sudan. Large swarms such as the ones that appeared over Kenya can eat the same amount of food as 80 million people in a single day, and affected areas can experience the total loss of crops and fodder. Sustained locust reproduction is expected until June 2020 and "represents an unprecedented threat to food security and livelihoods in the region, and could lead to further suffering, displacement and potential conflict".[108,109]

---

[101] United Nations Office for the Coordination of Humanitarian Affairs (OCHA), *Sahel: Overview of Humanitarian Needs and Requirements 2018*, https://reliefweb.int/sites/reliefweb.int/files/resources/Sahel%20HNRO%202018.pdf, p.3.

[102] Based on World Bank data available at https://data.worldbank.org/indicator: the percentage of population living below US$1.90 a day (2011 PPP) was multiplied by total population numbers in Ethiopia, Kenya, South Sudan and Uganda; data for Somalia is excluded from the estimate, as no poverty headcount ratio is available.

[103] International Organization for Migration (IOM), https://displacement.iom.int/reportsregion-move-%E2%80%94-mid-year-mobility-overview-january-june-2019?close=true.

[104] IOM, https://displacement.iom.int/reports/region-move-%E2%80%94-mid-year-mobility-overview-january-june-2019?close=true.

[105] OCHA, https://reliefweb.int/report/somalia/somalia-floods-update-un-ocha-noaa-echo-daily-flash-26-november-2019.

[106] FAO, 2020: *Early Warning Early Action Report on Food Security and Agriculture* (January-March 2020), Rome, http://www.fao.org/3/ca7557en/ca7557en.pdf.

[107] FAO, *Crop Prospects and Food Situation, December 2019*, http://www.fao.org/3/ca7236en/ca7236en.pdf.

[108] FAO, http://www.fao.org/emergencies/crisis/desertlocust/intro/en/.

[109] FAO, 2020: GIEWS Special Alert 347: The worst desert locust outbreak in decades threatens food security across East Africa, Rome, http://www.fao.org/3/ca7610en/ca7610en.pdf, and OCHA, 2020: Eastern Africa Region: Regional Floods and Locus Outbreak Snapshot, https://reliefweb.int/sites/reliefweb.int/files/resources/ROSEA_20200117_EasternAfrica_Flood_Snapshot_Jan2020_def.pdf.

Dataset references

GREENHOUSE GASES

World Data Centre for Greenhouse Gases:

WMO Greenhouse Gas Bulletin, No.15, November 2019, https://gaw.kishou.go.jp/.

Mauna Loa CO_2:

Keeling, C. D.et al., 1976: Atmospheric carbon dioxide variations at Mauna Loa Observatory, Hawaii. *Tellus*, 28, doi:10.1111/j.2153-3490.1976.tb00701.x.

Dr Pieter Tans, US National Oceanic and Atmospheric Administration/Earth System Research Laboratory (www.esrl.noaa.gov/gmd/ccgg/trends/) and Dr Ralph Keeling, Scripps Institution of Oceanography (scrippsco2.ucsd.edu/), University of California San Diego.

Cape Grim, Tasmania CO_2:

Cape Grim Baseline Air Pollution Station (CGBAPS), https://www.csiro.au/en/Research/OandA/Areas/Assessing-our-climate/Latest-greenhouse-gas-data

SURFACE TEMPERATURE

HadCRUT:

Morice, C. P. et al., 2012: Quantifying uncertainties in global and regional temperature change using an ensemble of observational estimates: The HadCRUT4 dataset, *Journal of Geophysical Research*, 117, doi:10.1029/2011JD017187.

NOAAGlobalTemp:

Zhang, H.-M. et al., NOAA Global Surface Temperature Dataset (NOAAGlobalTemp), Version 5. NOAA National Centers for Environmental Information, doi:10.25921/9qth-2p70 [8 January 2020].

GISTEMP:

GISTEMP Team, 2019: GISS Surface Temperature Analysis (GISTEMP), version 4. NASA Goddard Institute for Space Studies, https://data.giss.nasa.gov/gistemp/.

Lenssen, N. et al., 2019: Improvements in the GISTEMP uncertainty model. *Journal of Geophysical Research: Atmospheres,* 124 (12), doi:10.1029/2018JD029522.

ERA5

Hersbach, H. and al., 2019: The ERA5 global reanalysis. Under review at the *Quarterly Journal of the Royal Meteorological Society*.

JRA-55

Kobayashi, S. et al., 2015: The JRA-55 reanalysis: General specifications and basic characteristics. *Journal of the Meteorological Society of Japan*. Ser. II, 93(1).

CARBON BUDGET

Friedlingstein, P. et al., 2019: Global Carbon Budget 2019, *Earth System Science Data*, 11, https://doi.org/10.5194/essd-11-1783-2019.

OZONE

NASA Ozonewatch, https://ozonewatch.gsfc.nasa.gov/.

OCEAN HEAT CONTENT

Ishii, M. et al., 2017: Accuracy of global upper ocean heat content estimation expected from present observational data sets. SOLA 13, doi: 10.2151/sola.2017-030.

Cheng, L. et al., 2017: Improved estimates of ocean heat content from 1960 to 2015. *Science Advances*, 3(3), doi: 10.1126/sciadv.1601545.

Good, S. A. et al., 2013: EN4: quality controlled ocean temperature and salinity profiles and monthly objective analyses with uncertainty estimates. *Journal of Geophysical Research: Oceans*, 118, doi: 10.1002/2013JC009067.

Levitus, S. et al., 2012: World ocean heat content and thermosteric sea level change (0–2000 m), 1955–2010. *Geophysical Research Letters*, 39, doi: 10.1029/2012GL051106.

Roemmich, D. and J. Gilson, 2009: The 2004–2008 mean and annual cycle of temperature, salinity, and steric height in the global ocean from the Argo Program. *Progress in Oceanography*, 82(2), https://doi.org/10.1016/j.pocean.2009.03.004.

Hosoda, S. et al., 2008: A monthly mean dataset of global oceanic temperature and salinity derived from Argo float observations. Japan Agency for Marine-Earth Science and Technology (JAMSTEC) Rep. Res. Dev., Volume 8, http://www.jamstec.go.jp/ARGO/argo_web/ancient/MapQ/Hosoda_etal_MOAA_GPV.pdf.

von Schuckmann, K. and P.-Y. Le Traon, 2011: How well can we derive Global Ocean Indicators from Argo data? *Ocean Science*, 7, https://doi.org/10.5194/os-7-783-2011.

MARINE HEATWAVES

Hobday, A.J. et al., 2018 : Categorizing and naming marine heatwaves. *Oceanography* 31(2), https://doi.org/10.5670/oceanog.2018.205.

Optimum Interpolation Sea Surface Temperature (OISST)

Banzon, V. et al.,2016: A long-term record of blended satellite and in situ sea-surface temperature for climate monitoring, modeling and environmental studies. *Earth System Science Data*, 8, doi:10.5194/essd-8-165-2016

SEA LEVEL

Archiving, Validation and Interpretation of Satellite Oceanographic data (AVISO):

Legeais, J.-F. et al., 2018: An improved and homogeneous altimeter sea level record from the ESA Climate Change Initiative. Earth System Science Data, 10, doi: 10.5194/essd-10-281-2018

Copernicus Marine Environment Monitoring Service (CMEMS):

Pujol, M.-I. et al., 2016: DUACS DT2014: the new multi-mission altimeter data set reprocessed over 20 years. *Ocean Science*, 12, doi: 10.5194/os-12-1067-2016, 2016.

Ablain, M. et al, 2017: Satellite altimetry-based sea level at global and regional scales. *Surveys in Geophysics*, 38, doi: 10.1007/s10712-016-9389-8.

Escudier, P. A. et al., 2017: Satellite radar altimetry: principle, accuracy and precision. In *Satellite Altimetry Over Oceans and Land Surfaces* (D. Stammer and A. Cazenave, eds).

OCEAN pH

HOT Hawaii Ocean Time Series

Adapted from: Dore, J.E. et al., 2009: Physical and biogeochemical modulation of ocean acidification in the central North Pacific. Proceedings of the National Academy of Sciences of the United States of America, 106:12235-12240.

New Zealand series

https://marinedata.niwa.co.nz/nzoa-on/

Vance, J. et al., 2019: NZOA-ON: The New Zealand Ocean Acidification Observing Network. *Marine and Freshwater Research*, doi: 10.1071/MF19222.

SEA ICE EXTENTS

OSI-SAF v2:

Lavergne, T. et al., 2019: Version 2 of the EUMETSAT OSI SAF and ESA CCI sea-ice concentration climate data records. *The Cryosphere*, 13, doi:10.5194/tc-13-49-2019, 2019.

EUMETSAT Ocean and Sea Ice Satellite Application Facility (OSI SAF), 2017: Global sea ice concentration climate data record v2.0, doi: 10.15770/EUM_SAF_OSI_0008.

National Snow and Ice Data Center (NSIDC):

Fetterer, F. et al., 2017: Sea Ice Index, Version 3. NSDIC, doi: https://doi.org/10.7265/N5K072F8. [4 February 2020].

GLACIER AND ICE-SHEET MASS BALANCE

World Glacier Monitoring Service (WGMS):

World Glacier Monitoring Service (2019): Fluctuations of Glaciers Database, doi:10.5904/wgms-fog-2019-12. Online access: http://dx.doi.org/10.5904/wgms-fog-2019-12.

PRECIPITATION

Global Precipitation Climatology Centre (GPCC):

Ziese, M. et al., 2011: GPCC First Guess Product at 1.0°: Near-real-time first guess monthly land-surface precipitation from rain gauges based on SYNOP data, doi: 10.5676/DWD_GPCC/FG_M_100.

Schneider, U. et al, 2018: GPCC Monitoring Product: Near-real-time monthly land-surface precipitation from rain gauges based on SYNOP and CLIMAT data, doi: 10.5676/DWD_GPCC/MP_M_V6_100, http://dx.doi.org/10.5676/DWD_GPCC/MP_M_V6_100.

Schneider, U. et al., 2018: GPCC Full Data Monthly Product Version 2018 at 1.0°: Monthly land-surface precipitation from rain gauges built on GTS-based and historical data, doi: 10.5676/DWD_GPCC/FD_M_V2018_100.

EXTREMES INDICES

Schamm, K. et al., 2013: GPCC First Guess Daily Product at 1.0°: Near-real-time first guess daily land-surface precipitation from rain gauges based on SYNOP data, doi: 10.5676/DWD_GPCC/FG_D_100.

Ziese, M. et al., 2018: GPCC Full Data Daily Version.2018 at 1.0°: Daily land-surface precipitation from rain gauges built on GTS-based and historical data, doi: 10.5676/DWD_GPCC/FD_D_V2018_100.

WILDFIRE

Global Fire Assimilation System (GFAS)

Kaiser, J.W. et al., 2012 : Biomass burning emissions estimated with a global fire assimilation system based on observed fire radiative power. *Biogeosciences,* 9(1), https://confluence.ecmwf.int/display/CKB/CAMS%3A+Global+Fire+Assimilation+System+%28GFAS%29+data+documentation.

List of contributors

WMO MEMBERS

Algeria, Argentina, Armenia, Austria, Bangladesh, Bulgaria, Cameroon, Canada, Chile, China, Costa Rica, Côte d'Ivoire, Croatia, Cyprus, Denmark, Estonia, Finland, France, Georgia, Germany, Greece, Guinea, India, Indonesia, Iran (Islamic Republic of), Ireland, Israel, Italy, Japan, Jordan, Kazakhstan, Kenya, Latvia, Libya, Luxembourg, North Macedonia, Malaysia, Republic of Moldova, Morocco, Netherlands, New Zealand, Nigeria, Philippines, Poland, Russian Federation, Senegal, Serbia, Singapore, Slovakia, Slovenia, South Africa, Spain, Sudan, Sweden, Switzerland, Tajikistan, Tanzania, Trinidad and Tobago, Tunisia, Turkey, Ukraine, United Kingdom, United States, WMO RA VI Regional Climate Centre (RCC).

DATA CENTRES

Global Precipitation Climatology Centre (GPCC); Met Office Hadley Centre; National Oceanic and Atmospheric Administration National Centres for Environmental Information (NOAA NCEI); European Centre for Medium-range Weather Forecasts (ECMWF) and Copernicus Climate Change Service (C3S); National Aeronautics and Space Administration Goddard Institute for Space Studies (NASA GISS); Japan Meteorological Agency (JMA); WMO Global Atmospheric Watch (GAW); NOAA National Ocean Data Center (NODC); National Snow and Ice Data Center (NSIDC); Mauna Loa Observatory; the Blue Carbon Initiative; Hong Kong Observatory; Pan-Arctic Regional Climate Outlook Forum (PARCOF); European Space Agency (ESA) Climate Change Initiative (CCI); Copernicus Marine Environmental Monitoring Service (CMEMS); Archiving, Validation and Interpretation of Satellite Oceanographic data (AVISO); the Polar Portal; Department of Physical Oceanography, Woods Hole Oceanographic Institution; Arctic and Antarctic Research Institute (AARI); Mercator Ocean; Global Ocean Oxygen Network (GO2NE); Global Ocean Acidification Observing Network (GOA-ON); Ocean and Sea Ice Satellite Application Facility (OSISAF) of European Organisation for the Exploitation of Meteorological Satellites (EUMETSAT); Australian Bureau of Meteorology; Commonwealth Scientific and Industrial Research Organisation (CSIRO) Oceans and Atmosphere.

UNITED NATIONS AGENCIES

Food and Agriculture Organization of the United Nations (FAO), Intergovernmental Oceanographic Commission of the United Nations Educational, Scientific and Cultural Organization (IOC/UNESCO), International Monetary Fund (IMF), International Organization for Migration (IOM), United Nations Conference on Trade and Development (UNCTAD), United Nations Environment Programme (UNEP), Office of the United Nations High Commissioner for Refugees (UNHCR), United Nations Office for Disaster Risk Reduction (UNDRR), World Health Organisation (WHO).

INDIVIDUAL CONTRIBUTORS

PHYSICAL ASPECTS

Robbie Andrew (CICERO), Lynette Bettio, Pep Canadell (CSIRO), Anny Cazanave (Laboratoire d'Etudes en Géophysique et Océanographie Spatiales CNES and Observatoire Midi-Pyrénées, France), Robert Dunn (Met Office, UK), Pierre Friedlingstein (University of Exeter), Karsten Haustein (Oxford University, UK), Peer Hechler (WMO), Jennifer Howard (Conservation International), Matthias Huss (University of Fribourg, Switzerland), Kirsten Isensee (Intergovernmental Oceanographic Commission of the United Nations Educational, Scientific and Cultural Organization), Rob Jackson (Stanford University), John Kennedy (Met Office, UK), Rachel Killick (Met Office, UK), Takuji Kubota, Yuriy Kuleshov, Toshiyuki Kurino, Lisa Levin (Scripps), Patrick Megonigal (Smithsonian

Environmental Research Center), Glen Peters (CICERO), Corinne Le Quere (UEA), Robert W Schlegel (Department of Physical Oceanography, Woods Hole Oceanographic Institution, US), Katherina Luise Schoo (Intergovernmental Oceanographic Commission of the United Nations Educational Scientific and Cultural Organization), Karina von Schuckmann (Mercator Océan International, France), Vasily Smolyanitsky (Arctic and Antarctic Research Institute, Russian Federation), Martin Stendel (Danish Meteorological Institute, Denmark), Oksana Tarasova (GAW WMO), Tomoko Tashima, Blair Trewin (Bureau of Meteorology, Australia), Freja Vamborg (ECMWF and C3S), Pingping Xie, Michael Zemp (Switzerland), Markus Ziese (Deutscher Wetterdienst, Germany).

CLIMATE RELATED RISKS AND IMPACTS

Pierre Boileau (UNEP), Alessandro Costantino (FAO), Florence Geoffroy (UNHCR), Sarah Graf (FAO), Lorenzo Guadagno (IOM), Dina Ionesco (IOM), Kirsten Isensee (IOC-UNESCO), Maarten Kappelle (UNEP), Isabelle Michal (UNHCR), Lev Neretin (FAO), Oscar Rojas (FAO), Pinya Sarasas (UNEP), Jeremy Schlickenrieder (FAO), Joy Shumake-Guillemot (WHO/WMO)

ALSO CONTRIBUTED

Sandra Amlang (UNDRR), Diarmid Campbell Lendrum (WHO), Atsushi Goto (JMA), Katherine Hill (GCOS/GOOS), Clare Nullis (WMO), Wilfran Moufouma Okia (WMO), Mxolisi Shongwe (IPCC Secretariat), Michael Sparrow (WCRP), Yanchun Zhang (UNCTAD), Zinta Zommers (UNDRR), Peter Bissolli (DWD).

For more information, please contact:

World Meteorological Organization

7 bis, avenue de la Paix – P.O. Box 2300 – CH 1211 Geneva 2 – Switzerland

Stragegic Communications Office
Cabinet Office of the Secretary-General

Tel: +41 (0) 22 730 83 14 – Fax: +41 (0) 22 730 80 27

Email: cpa@wmo.int

public.wmo.int

JN 20127